Johannes Gutenberg-University Mainz

Faculty of Biology

Interleukin-4 receptor pathway in neurons

A doctoral dissertation

submitted in partial fulfillment

of the requirements for the degree of

doctor rerum naturalium

by

Steffen Lerch

born on 10th september
in Darmstadt

Mainz, 2018

The present thesis has been drafted in the period between June 2013 and May 2018 in the work group Neuroimmunology. Department of Neurology, University Medical Center Mainz

I hereby declare that I wrote the dissertation submitted without any unauthorized external assistance and used only sources acknowledged in the work. All textual passages which are appropriated verbatim or paraphrased from published and unpublished texts as well as all information obtained from oral sources are duly indicated and listed in accordance with bibliographical rules. In carrying out this research, I complied with the rules of standard scientific practice as formulated in the statutes of Johannes Gutenberg-University Mainz to insure standard scientific practice.

_____

Signature of Author

Contents

Abstract

Direct neuronal interleukin-4 receptor signaling in the context of neuroinflammation

Multiple sclerosis (MS) is a chronic demyelinating inflammatory disease of the central nervous system (CNS) and belongs to the most frequent causes of irreversible disability in younger people. During the disease course of MS and the corresponding animal model experimental autoimmune encephalomyelitis (EAE), both adaptive and innate immune cells infiltrate the CNS and initiate a progressing neuroinflammation. Especially during the progressive phase of chronic neuroinflammation, axonal degeneration is the main cause of disability. Previous experiments provided evidence for beneficial effects of T helper 2 lymphocytes (T_H2) in experimental neurotrauma. T cell-mediated neuroprotection after CNS injury occurred independently of T cell receptor signaling and was mediated through T_H2-derived interleukin-4 (IL-4), which potentiated neurotrophin signaling to injured neurons. In this thesis, it is shown that different IL-4 receptor (IL-4R) types exist on murine cortical neurons *in vitro*, which can be activated by IL-4 treatment and support neuron survival after excitotoxic insult. Moreover, all data of the group indicate evidence for a fast and direct neuronal IL-4R signaling pathway in neurons *via* IRS1-PI3K-PKC signal transduction, independently of neurotrophin signaling. IL-4R signaling pathway leads to cytoskeletal remodeling and axonal repair. Together, these findings demonstrate that IL-4 mediates neuroprotection and axonal regeneration of the injured CNS and leads the way to future clinical treatment strategies to repair axonal damage in chronic neuroinflammation, CNS injury or neurodegeneration.

Zusammenfassung

Der direkte, neuronale Interleukin-4-Rezeptor Signalweg im Kontext der Neuroinflammation

Multiple Sklerose (MS) ist eine chronisch verlaufende, demyelinisierende und inflammatorische Erkrankung des Zentralen Nervensystems (ZNS). Sie ist die häufigste Ursache von irreversiblen Behinderungen junger Menschen. Sowohl bei MS als auch im vergleichbaren Versuchstiermodell, der experimentellen autoimmunen Enzephalomyelitis, infiltrieren Zellen des adaptiven und des angeborene Immunsystems das ZNS und verursachen eine fortschreitende Nervendegeneration. Körperliche Ausfälle und Einschränkungen werden hierbei durch die fortschreitende axonale Beschädigung ausgelöst. Die Arbeitsgruppe von Walsh und Kollegen konnten bisher zeigen, dass Lymphozyten des Typs T_H2 einen förderlichen Effekt auf die geschädigten Neuronen haben. Darüber hinaus waren sie in der Lage zu zeigen, dass dieser neuroprotektive Effekt von T Zellen unabhängig einer T Zellrezeptor-Aktivierung erfolgen kann. Gesteuert wird dies durch das T_H2 spezifische Interleukin-4 (IL-4), welches die Neurotrophinsignaltransduktion verstärkt. In der vorliegenden Arbeit wird gezeigt, dass es verschiedene IL-4 Rezeptoren (IL-4R) auf *in vitro* kultivierten kortikalen Neuronen präsentiert werden und durch die Behandlung mit IL-4 aktiviert werden können. Zudem zeigen alle Daten der Gruppe, dass es einen IL-4-spezifischen Signalweg in Neuronen gibt, welcher die Aktivierung der IRS1-PI3K-PKC unterliegt und einer Steigerung der Regeneration und des Auswachsens von Neuronen führt und unabhängig von der Verstärkung durch Neurotrophine abläuft. Mit Hilfe von immunozytochemischer Färbungen des filamentären Aktins in Neuronen, unter verschiedenen Behandlungen war es möglich, die Auswirkungen der IL-4R Signalkaskade auf die Remodelierungsprozesse des Zytoskeletts darzustellen. Zusammengefasst zeigen die Daten dieser Arbeit, dass IL-4 sowohl neuroprotektiv wirkt, als auch positiven Einfluss auf die axonale Regeneration hat. Hiermit wird der Grundstein für zukünftige Bestrebungen nach einer klinischen Behandlung für Nervenschäden und chronische, neuroinflammatorische Erkrankungen gelegt.

Publication List

The following publications have been achieved during this doctoral thesis:

"Fast direct neuronal signaling via the IL-4 receptor as therapeutic target in neuroinflammation"

C. F. Vogelaar*, Shibajee Mandal*, **Steffen Lerch***, Katharina Birkner, Jerome Birkenstock, Ulrike Bühler, Andrea Schnatz, Cedric S. Raine, Stefan Bittner, Johannes Vogt, Jonathan Kipnis, Frauke Zipp
Science Translational Medicine, 2018
PMID: 29491183

*equally contributing authors

"Growing the corticospinal tract: CNS regeneration in the culture dish"

Andrea Schnatz*, **Steffen Lerch***, Carine Thalman, Christina F. Vogelaar
In preparation

"FTY720 (fingolimod) treatment tips the balance towards less immunogenic antigen-presenting cells in patients with multiple sclerosis"

Felix Luessi, Stefan Kraus, Bettina Trinschek , **Steffen Lerch**, Robert Ploen, Magdalena Paterka, Torsten Roberg, Laura Poisa-Beiro, Luisa Klotz, Heinz Wiendl, Tobias Bopp, Helmut Jonuleit, Valerie Jolivel, Frauke Zipp and Esther Witsch
Multiple Sclerosis, 2015
PMID: 25732840

"Cladribine exerts an immunomodulatory effect on human and murine dendritic cells"

Stefan Kraus, Felix Luessi, Bettina Trinschek, **Steffen Lerch**, Mario Hubo, Laura-Poisa-Beiro, Magdalena Paterka, Helmut Jonuleit, Frauke Zipp, Valerie Jolivel
Int Immunopharmacol. 2013
PMID: 24316255

1. **Introduction**

1.1 Multiple sclerosis

Multiple sclerosis (MS) is a chronic demyelinating inflammatory disease of the central nervous system (CNS) representing one of the most common causes of disability in young people. It is a disorder of the brain and spinal cord in which focal infiltration of lymphocytes leads to damage of the myelin sheath and, as a consequence, the axon itself (Compston and Coles 2008). Typical first manifestations of MS symptoms are paresthesia, visual disturbances, ataxia and muscle weakness resulting from slowly progressing breakdown of nerve tissue. In most patients, MS emerges with a relapsing-remitting (RR-MS) clinical course characterized by inflammatory attacks and resulting myelin destruction, leading to yet reversible neurologic dysfunction. After initial relapses, inflammatory attacks are intermitted with variable periods of partial recovery (Figure 1). Approximately 30-60% of RR-MS patients develop a significant disease progression and convert to a secondary progressing form of MS (Larochelle, Uphaus et al. 2016). Secondary progressive MS (SP-MS) shows a steady increase in the patient's disability accompanied by CNS atrophy and neurodegeneration (Figure 1). The age of onset of progression is around 40 years whereas 38% do not develop progression by the age of 75 (Tutuncu, Tang et al. 2013). Early indicators of SP-MS are subtle but patients experience an overall worsening while only little changes in neurological examination can be observed (Larochelle, Uphaus et al. 2016). Nevertheless, compared to RR-MS patients with disease duration of more than 10 years, SP-MS patients display a 2-10-fold increased chance of experiencing impairments of cognitive functions representing higher-order network changes (Huijbregts, Kalkers et al. 2004, Planche, Gibelin et al. 2016). The third and rather rare form of MS is called primary progressive (PP)-MS which does not include classical relapse events and is characterized by a steady disease progression (Lublin and Reingold 1996).

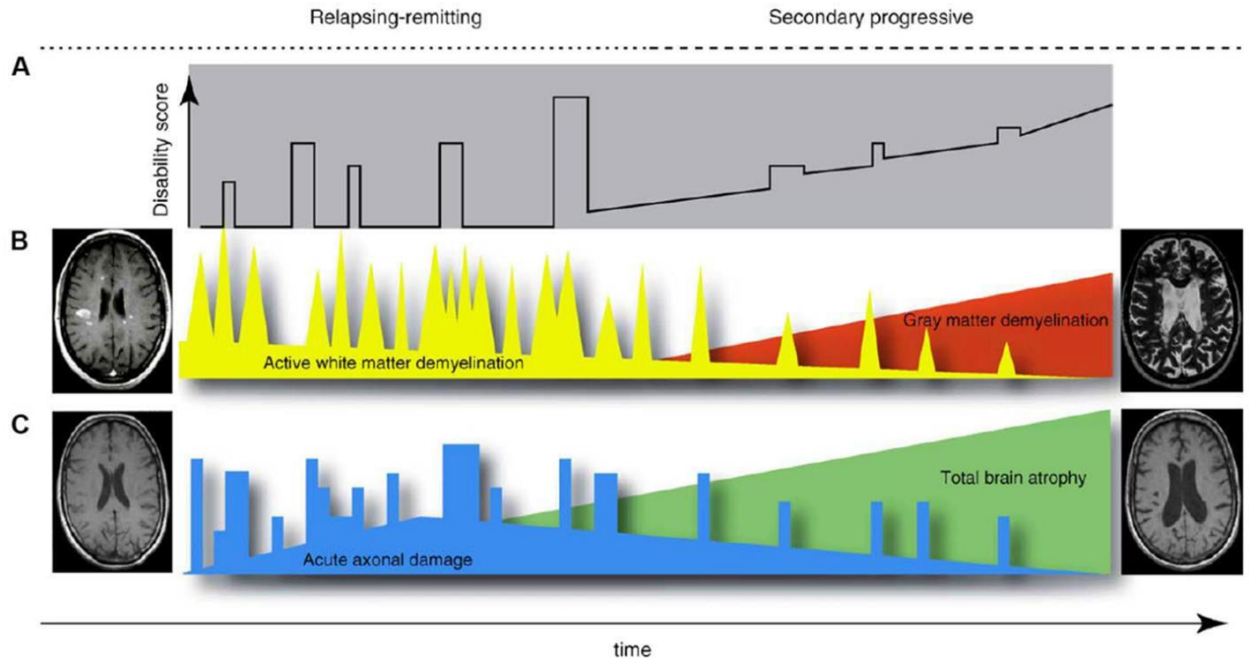

Figure 1: Disease progression in multiple sclerosis (Siffrin, Vogt et al. 2010)

A The relapsing remitting MS course progresses into a secondary progressive form leading to increasing disability. **B** Active white matter demyelination occurs in the relapsing remitting phase with highly frequent attacks and converts to a steadily increasing grey matter demyelination in the secondary progressive phase. **C** The acute white matter demyelination progresses to axonal damage and leads to a phase of severe brain tissue atrophy accompanied by disability.

MS is mainly driven by autoreactive inflammatory lymphocytes invading the CNS and initiating the destruction of myelin sheath, leading to the damage of the neuronal compartment (Herz, Zipp et al. 2010, Sawcer 2011). However, there is increasing evidence that axons are attacked independent of demyelination (Nikic, Merkler et al. 2011)

1.1.1 Neuronal loss and dysfunction in MS

The progressive neurodegeneration caused by inflammation and characterized by axonal loss and neuronal damage plays a main role in MS (Vogt, Paul et al. 2009). In phases of inflammatory attacks, axons undergo pathological swellings, which are reversible (Nikic, Merkler et al. 2011). Magnetic resonance imaging (MRI) and electrophysiology have been used to visualize demyelination and neurodegeneration in patients, showing severe tissue

destruction and neuronal loss as so-called black holes on the T1-weighted spin-echo. These longitudinal scans reflect the development of MS by visualizing new lesions and therefore new inflammatory processes, which end in the breakdown of the blood-brain barrier. The CNS bears a limited capacity to maintain the process of re-myelination and even has the potential to achieve the full clinical remission (Franklin and Ffrench-Constant 2008). As soon as an axon is completely transected or the integrity of a neuronal cell body is damaged, the mechanisms of the CNS are insufficient to repair the damage and the cells undergo apoptosis (Siffrin, Radbruch et al. 2010, Nikic, Merkler et al. 2011).

In the CNS, numerous molecular changes occur upon inflammation, eventually leading to neuronal degeneration (Friese, Schattling et al. 2014). The loss of axons and neurons following demyelination then leads to the MS-specific characteristics. CNS-infiltrating immune cells have been shown to secrete neurotoxic molecules, e.g. reactive oxygen species (ROS), glutamate and chemokines, initiating immune responses. The relationship between inflammatory lesions, demyelination and the neurodegenerative changes is still not fully understood. The loss of trophic support from oligodendrocytes, occurring during demyelination, promotes axonal degeneration by impairment of mitochondrial functions. This leads to a reduced adenosine tri-phosphate (ATP) production, thereby causing a focal transport blockage and axonal swelling (Ferreirinha, Quattrini et al. 2004). However, degeneration of neurons and axonal loss can also occur without local demyelination (Funfschilling, Supplie et al. 2012).

Due to the complexity of MS and the limited access to human material, it is not surprising that most of our current knowledge about neurodegeneration in MS originates from experimental autoimmune encephalomyelitis (EAE) (Friese, Schattling et al. 2014). This animal model of MS mimics many clinical and neuropathological features of the human disease (Friese, Montalban et al. 2006). When identifying neurodegenerative pathways in MS or EAE, one must be aware of indirect effects of inflammatory processes (Friese, Schattling et al. 2014).

1.1.2 Experimental autoimmune encephalomyelitis (EAE) as animal MS model

EAE was first introduced in 1933 by Rivers et al., who started experimenting on monkeys by immunization with rabbit brain emulsion to introduce disseminated lesions (Rivers, Sprunt et al. 1933). To date, the most commonly used are mouse EAE models which show several clinical parallels to human MS patients, such as demyelination, inflammation, paralysis and weight loss (Ransohoff 2012). However, EAE can only reflect a small part of the huge clinical spectrum of MS symptoms and the various forms it can take.

In general, two types of EAE models are used, active EAE and passive transfer EAE. Relevant for this thesis is active EAE, involving immunization with a protein or peptide whereas for the initiation of a passive EAE encephalitogenic T cells are transferred to the mice. For active immunization, the immunogen myelin oligodendrocyte glycoprotein (MOG_{35-55}) is injected into C57BL/6 mice and proteolipid protein (PLP) is injected into SJL mice in combination with complete Freud's adjuvant (CFA) (Figure 2) (Laatsch, Kies et al. 1962, Tuohy, Sobel et al. 1992). CFA contains mineral oil and inactivated mycobacteria, which are both recognized by Toll-like receptors (TLR) and trigger a strong inflammatory reaction. With an additional intraperitoneal injection of pertussis toxin (PTX), the permeability of the blood-brain barrier is increased, acting through an induced angiogenesis in the brain microvascular endothelial cells (Lu, Pelech et al. 2008).

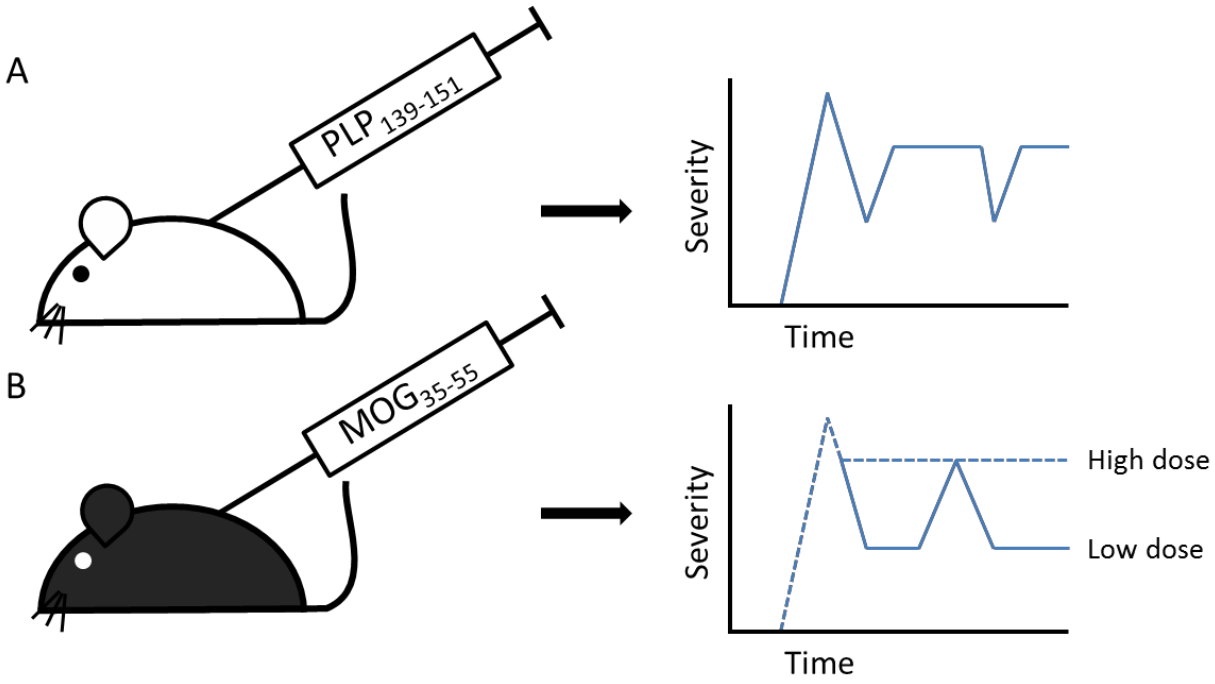

Figure 2: Schematic view of the variations in active EAE immunization and resulting disease course (adopted from (Rangachari and Kuchroo 2013)

A Immunization of SJL/J mice with $PLP_{139-151}$ resulting in an initial paralytic EAE phase, followed by multiple remissions and relapses. **B** Immunization of B6 mice with MOG_{35-55} causing a chronic disease course with no release after the initial attack peak.

The different combinations of mouse strains and peptides reflect different types of EAE courses after immunization. The administration of MOG_{35-55} peptide in C57BL/6 mice induces a chronic EAE (Tompkins, Padilla et al. 2002), whereas the immunization with $PLP_{139-151}$ tends to provoke a relapsing-remitting disease course (Tuohy, Sobel et al. 1992). The onset of classical EAE is a result of the preferential immune attack on the spinal cord. The progression of the EAE can be categorized in five different scores, starting with the development of an ascending paralysis at the tail (score 1), proceeding to the hind limbs (score 2) and forelimbs (score 3), leading to quadriplegia (score 4) and finally the death of the animal (score 5) The EAE model in combination with genetically modified strains is a powerful tool to study CNS demyelinating diseases, including MS, and to assess the influence of genetic engineering or for drug testing.

1.2 IL-4 signaling and IL-4R subtypes

1.2.1 Interleukin 4

In addition to pro-inflammation mechanisms, the immune system can also function to repress or limit inflammatory responses. The failure of the body to suppress the inflammation generally leads to damage to the organs or cells. It could lead to an inappropriate response to non-pathogenic foreign particles or commensal bacteria or generate/tolerate an inappropriate immune response to the organism itself (auto-immunity). Cytokines are small immune-modulating agents responsible to respond to these factors by binding to specific cytokine receptors and activate cell signaling pathways. In this context, interleukin-4 (IL-4) is a multifunctional cytokine that plays a critical role in the regulation of these immune responses (Nelms, Keegan et al. 1999). IL-4 is a pleiotropic type I cytokine produced by $CD4^+$ T_H2 cells, astrocytes, basophilic granulocytes and mast cells in response to activation (Seder and Paul 1994, Sholl-Franco, da Silva et al. 2009). Also γ/δ T cells and eosinophilic granulocytes have been reported to produce IL-4 (David A. Ferrick 1994, S Dubucquoi 1994). However, the endogenous IL-4 levels in mice are in the picogram per milliliter range (Hasan, Seo et al. 2016). During sub-lethal ischemia, neurons have been reported to synthesize IL-4 in small amounts which then modulate microglial function by polarizing microglia to an M2 phenotype (Zhao, Wang et al. 2015). Moreover, the regulation and differentiation of antigen-stimulated naïve T cells can be controlled by IL-4. It causes these cells to develop into T_H2 cells which are capable of producing even more IL-4 and other cytokines including IL-5, IL-10 and IL-13 (Hsieh CS1 1992, R A Seder 1992). A second function of IL-4 is the powerful suppression of the IFN-γ production in $CD4^+$ T cells.

The compact and globular folding structure of IL-4 is similar to other cytokines and stabilized by three disulfide bonds. IL-4 is a member of the 4 alpha-helix bundle family of cytokines with a left-handed twist dominating half of its structure (K. Izuhara 2002). The human IL-4 protein has a length of 153 amino acids whereas the murine sequence consists of 140 amino acids. The protein sequences share an identity of 40% which is remarkably low, compared to the similarity in function (Figure 3).

An understanding of how IL-4 mediates this wide range of effects requires the analysis of the function of the IL-4 receptor.

NW Score	Identities	Positives	Gaps
235	62/154(40%)	87/154(56%)	15/154(9%)

```
Query  1    MGLTSQLLPPLFFLLACAGNFVHGHKCDIT-LQEIIKTLNSLTEQKTLCTELTVTDIFAA  59
            MGL  QL+  L F L C  + +HG  CD   L+EII  LN +T + T CTE+ V ++  A
Sbjct  1    MGLNPQLVVILLFFLECTRSHIHG--CDKNHLREIIGILNEVTGEGTPCTEMDVPNVLTA  58

Query  60   SKNTTEKETFCRAATVLRQFYSHHEKDTRCLGATAQQFHRHKQLIRFLKRLDRNLWGLAG  119
            +KNTTE E  CRA+ VLR FY  H K T CL   +      ++L R  + LD ++
Sbjct  59   TKNTTESELVCRASKVLRIFYLKHGK-TPCLKKNSSVLMELQRLFRAFRCLDSSI-----  112

Query  120  LNSCPVKEANQSTLENFLERLKTIMREKYSKCSS  153
               SC + E+  ++L++FLE LK+IM+  YS
Sbjct  113  --SCTMNESKSTSLKDFLESLKSIMQMDYS      140
```

Figure 3: Protein BLAST of the human and murine IL-4

The protein sequences of human (Query) and murine (Sbjct) IL-4 share an identity of 40% and only show 9% gaps.

1.2.2 IL-4 receptor complex

The interleukin-4 receptor (IL-4R) is expressed on the surface of hematopoietic, endothelial, muscle, fibroblast, hepatic and brain cells (Nelms, Keegan et al. 1999). The IL-4R consists of a heterodimer formed by two chains and can be found in two different types. The bipartite IL-4R Type I comprise the IL-4Rα and the common-γ chain (γC), is found on hematopoietic cells and is activated by IL-4 only. Both receptor subunits belong to the cytokine receptor superfamily and are shared by other cytokines (Kammer, 1996; Bazan, 1990). The IL-4R Type II consists of the IL-4Rα and the IL-13Rα1 chain, is found on non-hematopoietic cells and can be activated by both IL-4 and IL-13 (Figure 4) (Heller, Dasgupta et al. 2012).

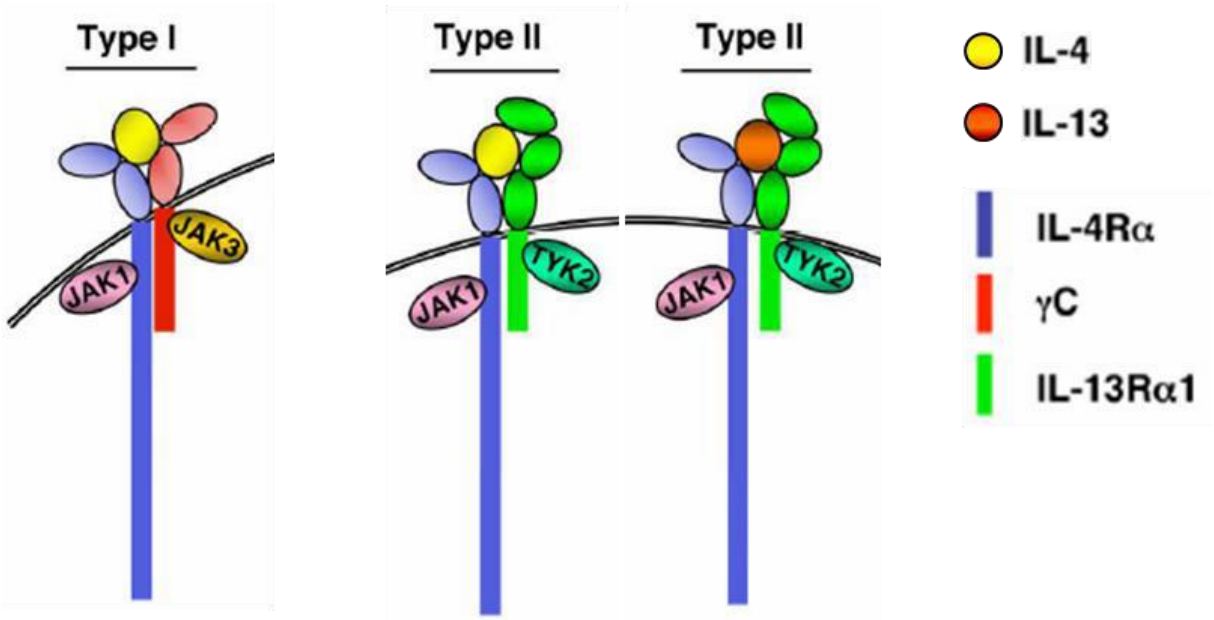

Figure 4: The IL-4R System (adapted from Heller et al. 2012 inTech)

Schematic drawings showing the functional IL-4R Type I and II. IL-4Rα binds with a high affinity to IL-4, resulting in a dimerization with the γC or IL-13Rα1 chain to form the Type I or Type II complex, respectively. In contrast, IL-13 binds with a lower affinity to the IL-13Rα1 chain of the Type II receptor complex. Ligand binding is followed by the activation of, among others, receptor-associated Janus Kinases (JAKs) for intracellular signaling.

Both IL-4R types are activated by the initial binding of the ligand to the IL-4Rα (Type I) and IL-13Rα chain (Type II) and subsequent recruiting of the second chain to form the complete receptor complex (Nelms, Keegan et al. 1999).

The IL-4Rα chain (CD124) is a 140 kDa protein and displays a broad distribution on hematopoietic and non-hematopoietic cells (PArk, Friend et al. 1987). It binds IL-4 with a very high affinity, with a *Kd* ranging between 20-300 pM (Lowenthal, Castle et al. 1988). The γC chain (CD132) is a 60 kDa protein that dimerizes with the IL-4Rα chain upon IL-4 binding to form the functional Type I receptor. It is also found in the composition of many other cytokine receptor complexes such as the IL-2, IL-7, IL-9, IL-15 and IL-21 receptors (Nelms, Keegan et al. 1999). The IL-13Rα1 chain (CD213a1) is a 65-70 kDa glycosylated protein which is encoded on the X-chromosome in human and mouse and can act either as a receptor for the IL-13 (*Kd* of around 30 nM) or heterodimerize with the IL-4Rα chain upon binding with the ligand IL-4 (Zurawski, Vega et al. 1993, Andrews, Holloway et al. 2002).

1.2.3 Activation of signal transduction by IL-4R

To date, it was shown exclusively in immune cells that the binding of IL-4 with the IL-4Rα initiates the recruitment with either one of the co-chains to form the heterodimeric IL-4R Type I or II (Kammer, Lishcke et al. 1996). The dimerization of the receptor complex leads to the activation of tyrosine kinases that phosphorylate cellular substrates and initiate signaling cascades (Miyajima, Kitamura et al. 1992). Janus kinases (Jak-1, Jak-2 and Jak-3) have been reported to be activated upon IL-4R complex activation (Johnston, Kawamura et al. 1994, Witthuhn 1994, Murata, D. et al. 1996). Jak-1 and Jak-2 are associated with the IL-4Rα1 chain, while Jak-3 is reported to associate with the γC chain (Miyazaki, Kawahara et al. 1994, Russell, Johnson et al. 1994, Murata, D. et al. 1996). Activation of these kinases leads to the phosphorylation of five conservative tyrosine residues in the cytoplasmic region of the IL-4Rα leading to subsequent interaction with downstream signaling proteins through the receptor docking protein Src-homology 2 (SHC2) (Smerz-Bertling and Duschl 1995). Generally, the IL-4Rα chain has three functionally distinct domains, one for interaction with Janus kinases, one for the activation of proliferative pathways and one for activation of pathways leading to the induction of gene expression (Nelms, Keegan et al. 1999).

Active parts of the proliferative IL-4R-mediated pathways are the insulin receptor substrate-1 and -2 (IRS-1/2). IRS-1 and 2 are closely related 170 kDa proteins and are phosphorylated upon activation of the IL-4R by IL-4 (Sun, Wang et al. 1995). Following the self-phosphorylation of Jak-1 and the subsequent phosphorylation of the IL-4Rα chain, IRS-1/2 interacts with the IL-4R motif. This interaction results in docking to the IL-4α chain which was shown by co-immunoprecipitation of the IL-4R after activation with IL-4 (Keegan 1994). Subsequently, IRS-1/2 become phosphorylated by the action of receptor-associated kinases as well (Jak-1,-2,-3) (Yin 1995). The IRS-1/2 docking proteins harbor approximately 20 potential sites for tyrosine phosphorylation which mostly bind to SH2 domains, giving a perspective over the broad potential of the IRS-1/2 as mediators of cytosolic signaling (Sun, Rothenberg et al. 1991, Sun, Wang et al. 1995). Furthermore, IRS-1/2 activate the MAPK signaling pathway by the interaction with phosphoinositide-3-kinase (PI3K) and the adapter molecule GRB-2 (Figure 5) (Nelms, Keegan et al. 1999).

1.2.4 The PI3K pathway

Phosphatidylinositol-4,5-biphosphate-3-kinase (PI3K) is part of the PI3K intracellular signal transducer family which represent a minor component of the plasma membrane and is linked to an extraordinarily diverse group of cellular functions, including cell growth, proliferation, differentiation, cellular motility and survival (Okkenhaug, 2013). PI3K consists of two subunits: A 85 kDa regulatory (p85) subunit with a triple phosphorylated inositol ring creating a docking site for proteins and a 110 kDa catalytic (p110) subunit (Leevers, 1999; Okkenhaug, 2013). Upon IL-4 stimulation, the p85 subunit acts as an adapter molecule to link p110 with one of the ten potential phosphorylated tyrosine molecules of IRS-1/2 (Sun, Wang et al. 1995). The interaction of PI3K with phosphorylated IRS-1/2 leads to a conformational change resulting in the activation of p110 which initiates the lipid kinase pathways to transfer phosphate from ATP to the inositol in phosphatidylinositol (Dhand, Hiles et al. 1994). Phosphoinositide ($Ins(3,4,5)PO_4$,) initiates the opening of membrane calcium channels and subsequently activates the downstream kinases protein kinase C (PKC) and the Akt kinase (Figure 5) (Franke, Kaplan et al. 1997).

1.2.5 PKC signaling

Protein kinase C (PKC) is a family of structurally related protein kinases that phosphorylate hydroxyl groups of serine and threonine amino acid residues of their target proteins. PKCs are essential for several signal transduction cascades and are activated by an intracellular increase in concentration of diacylglycerol or calcium ions (Ca^{2+}). The isotypes of PKCs are divided into three subgroups: conventional (α, β1, β2,γ), novel (δ, ε, η, Θ) and atypical (ι, ζ). This division is based on their involvement in different second messenger systems (Nishizuka 1995). The conventional PKC subgroup is activated by intracellular Ca^{2+}, whereas novel isoforms lack the C2 calcium-binding domain. The atypical isoforms lack both the C2 calcium binding and the DAG-binding domain. Regulation of the atypical PKC occurs in part through the N-terminal PB1 domain (Parker and Murray-Rust 2004). For all PKC isoforms the activation-resulting allosteric effect leads to a loss of the inhibiting pseudo-substrate sequence that otherwise occupies the active site (Parker and Murray-Rust 2004). Of the conventional PKCs, the γ subtype shows a

unique neuronal distribution and localization in the brain (Tanaka and Saito 1992). It is found in the spinal cord and the cerebral cortex and its location is restricted to neurons. Besides neuronal development, PKCγ's spectrum of cellular functions includes modulation of synaptic plasticity (long term potentiation (LTP), long term depression (LTD)) (Saito and Shirai 2002).

The positive contribution of PKC in signal transduction can be blocked by the staurosporine derivate bisindolylmaleimide I (Bis1). This compound competes with ATP for binding to PKC, thus interfering with the transfer of phosphate to PIP2 (DAvis, Hill et al. 1989). On the other hand, PKC pathways can be activated by the insulin-like growth factor 1 (IGF-1). Activation of the IGF-1 receptor results in the recruitment and phosphorylation of IRS-1/2 and Shc by the heterotetrameric transmembrane receptor tyrosine kinase (RTK), which then leads to an increased activation of PKCs.

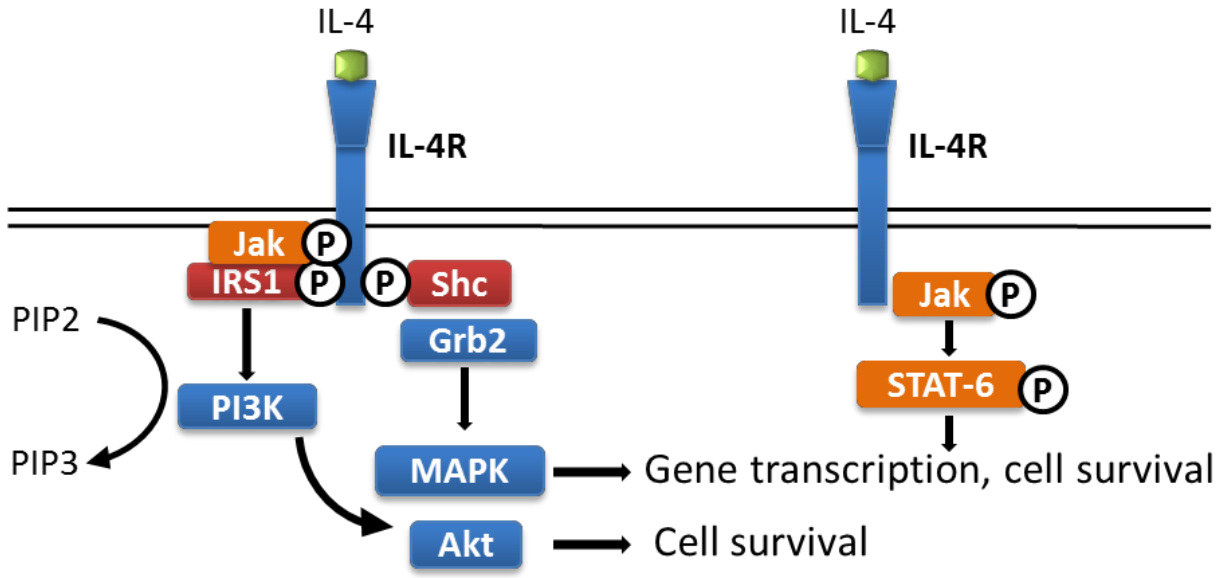

Figure 5: IL-4R signaling in lymphocytes

IL-4R signaling comprising the PI3K/Akt, MAPK/Erk, and Jak-STAT pathways known in lymphocytes (A. D. Keegan 1994). PI3K is activated by the IL-4R docking protein IRS-1 and subsequently converts PIP2 ($Ins(3,4)PO_4$)to PIP3 ($Ins(3,4,5)PO_4$) which opens membrane bound Ca^{2+} channels. The activation of these pathways leads to upregulation of gene transcription and cell survival.

1.2.6 GAP-43 in axonal regeneration

The growth-associated protein GAP-43, also known as neuromodulin, is a 43 kDa presynaptic protein that is mainly expressed in the nervous system (Woolf, Reynolds et al. 1992, Oestreicher, De Graan et al. 1997) Originally, GAP-43 was discovered in explorations to identify phosphoproteins of the synapse and later it was found to be involved in functions like formation of growth cones and the binding of CaM (Zwiers, Veldhuis et al. 1976, Katz, Ellis et al. 1985, De Graan, Oestreicher et al. 1990). The earliest expression of GAP-43 was shown in post-mitotic neurons with a high expression in the nervous system until it is down-regulated at synaptogenesis (Biffo, Verhaagen et al. 1990). After disruption of the nervous tissue architecture the expression of GAP-43 is reintroduced not only in neurons, but also in glial cells (Oestreicher, De Graan et al. 1997). Not only injury initiates an increase in expression of GAP-43, also alterations of synaptic efficacy elicited by LTP affect the phosphorylation state and the expression of GAP-43 (Meberg, Valcourt et al. 1995, Ramakers 1995).

In comparison to other CaM-binding proteins that are enriched in neuronal cells and require relatively high calcium concentrations, GAP-43 can bind to CaM at low ambient calcium concentrations (De Graan, Oestreicher et al. 1990). On the contrary, upon a rise of intracellular calcium above the ambient level, PKC gets activated and phosphorylates a specific serine residue of GAP-43 (Mahoney, Seki et al. 1995). This phosphorylation results in a conformational change in the GAP-43 protein structure and leads to the release of CaM, resulting in the activation of downstream actin-remodeling proteins like CamKII (Chapman, Douglas et al. 1990, Chapman, Estep et al. 1992). Subsequently, CamKII inactivates cofilin by phosphorylation. Active cofilin supports the depolymerisation of filamentous actin (F-actin) into globular actin (G-actin) at the negative end of actin fibers (Laux, Fukami et al. 2000). GAP-43 activates profilin, which triggers the polymerization of G-actin to F-actin at the positive end of the actin filaments (Kevenaar and Hoogenraad 2015). The composition of microtubules and neurofilaments and the organization of actin filaments are both important mechanisms of the cytoskeleton and required for the axonal formation and axonal transport. Moreover, regulation of these mechanisms is essential for the arrangement of several specialized axonal structures, such as the growth cones (Kevenaar and Hoogenraad 2015).

1.3 Aim of this study

Previously, our group demonstrated that T_H2 cells promote axonal regeneration and functional recovery after spinal cord injury (SCI). We were able to show that T_H2 cell-derived IL-4 protects and induces recovery of injured neurons. IL-4 potentiated the neurotrophin-3-induced activation of the Akt and MAPK pathways (Walsh, Hendrix et al. 2015). IL-4 may act via signaling pathways shared with neurotrophins through the activation of receptor adaptor proteins (Blaeser, Bryce et al. 2003). In previous *in vitro* studies, recombinant NT-3 was shown to potentiated spontaneous axonal outgrowth in organotypic hippocampal cultures (Hechler, Boato et al. 2010). Thus, the enhancement of neurotrophin signaling by IL-4 pre-incubation likely leads to the activation of axonal growth pathways. In line with these findings, IL-4R knock-out mice or mice with mutations in the IL-4 transduction cascade show impairment of axonal outgrowth (Walsh, Hendrix et al. 2015).

Although these investigations suggest a role of IL-4 in neuroprotection and -regeneration via potentiating neurotrophin signaling, a direct influence of IL-4 on neurons was not demonstrated conclusively yet. The aim of the lab´s overall study was to elucidate the direct impact of IL-4 on neuronal regeneration and to identify the signaling pathways that are activated by IL-4 in neurons. For this purpose, a hypothetical signaling pathway was designed based upon similarities between IL-4R signaling in immune cells and neurotrophin signaling in neurons (Figure 6). In this thesis, I describe data contributing to the finding of the group regarding a fast and direct neuronal IL-4R signaling pathway *in vitro*, which was eventually found to be responsible for neurite outgrowth and regeneration.

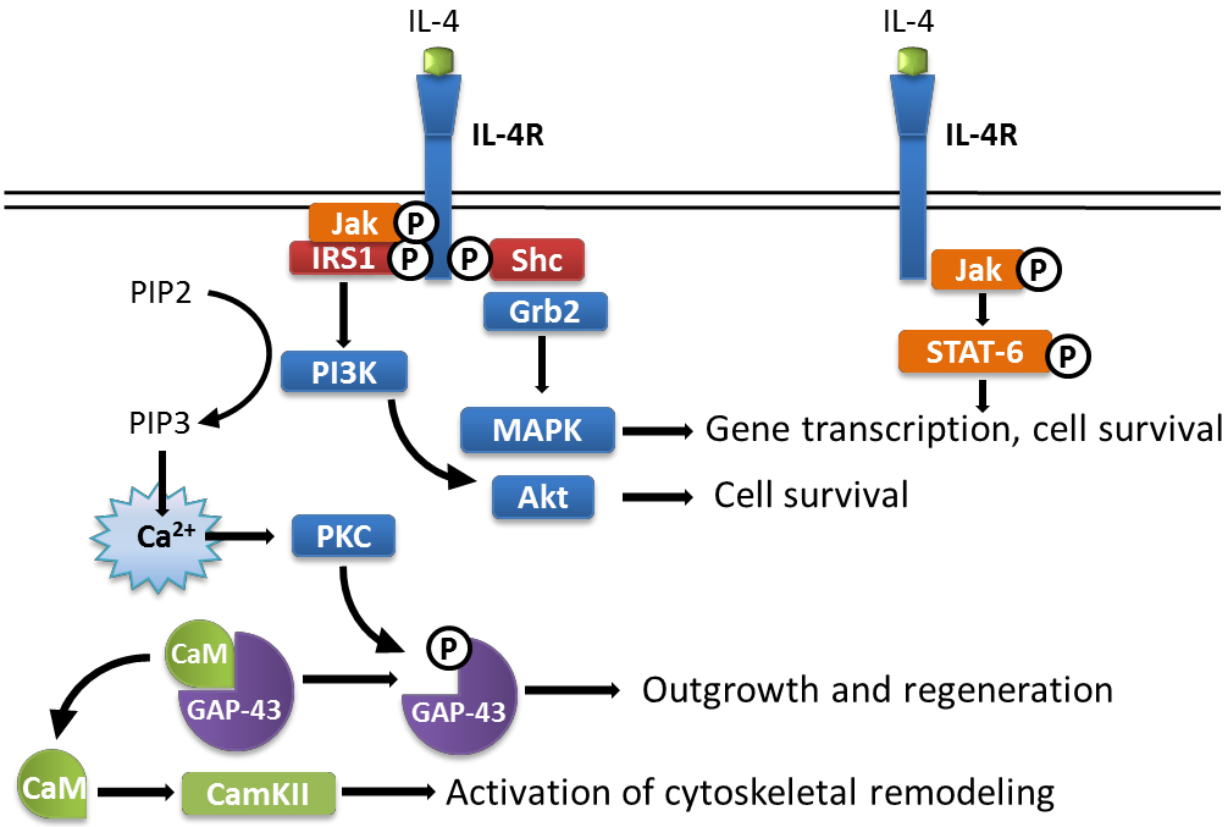

Figure 6: Hypothetical IL-4R signaling pathways in neurons, based upon Nelms, Keegan et al. 1999, Lee et al. 2001 and Oestreicher et al. 1997

Hypothesis of the potential IL-4R signaling in neurons comprising PI3K/PKC, Akt/MAPK, Jak/STAT and GAP-43. Based upon the similarities between IL-4R signaling in immune cells, and neurotrophin signaling in neurons these pathways would lead in neurons to an increased gene transcription, cell survival and activation of cytoskeletal remodeling processes and therefore to outgrowth and regeneration.

2. Materials and Methods

2.1 Materials

2.1.1 Chemicals and Buffers

Compound	Company
10x RotiBlock	Carl Roth GmbH, Karlsruhe (Germany)
β-Mercaptoethanol	Sigma-Aldrich Corp., St Louis (USA)
Albumin bovine, cell culture grade (BSA)	Serva Electrophoresis, Heidelberg (Germany)
Ammonium chloride (NH_4Cl)	Sigma-Aldrich Corp., St Louis (USA)
Aqua bi. dest. Sterile	B. Braun AG, Melsungen (Germany)
Calcium-chloride (CaCl2)	Carl Roth GmbH, Karlsruhe (Germany)
4,6-diamidino-2phenylindole, dihydrochloride (DAPI)	Thermo Fisher Scientific, Waltham (USA)
D-Glucose	Carl Roth GmbH, Karlsruhe (Germany)
D (+) Saccharose	Carl Roth GmbH, Karlsruhe (Germany)
Dextrose	Carl Roth GmbH, Karlsruhe (Germany)
Dithiothreitol (DTT)	Carl Roth GmbH, Karlsruhe (Germany)
Dimethyl Sulfoxide (DMSO)	Sigma-Aldrich Corp., St Louis (USA)
DNase I	F. Hoffmann-La Roche AG, Basel
Dulbeccos PBS with Ca^{2+} & Mg^{2+}	Gentaur, Kampenhout (Belgium)
Ethanol 100 % (v/v) (EtOH)	AppliChem GmbH, Darmstadt (Germany)
Ethanol 70 % (v/v) (EtOH)	AppliChem GmbH, Darmstadt (Germany)
Ethylenediaminetetraacetic acid (EDTA)	Carl Roth GmbH, Karlsruhe (Germany)
Fetal Bovine Serum, heat inactivated (FBS)(FCS)	Biochrom AG, Berlin (Germany)
Guanidine Hydrochloride	Carl Roth GmbH, Karlsruhe (Germany)
Glycine	Carl Roth GmbH, Karlsruhe (Germany)
HEPES	Life Technologies Corp., Grand Island (USA)
Horse Serum, heat inactivated	Thermo Fisher Scientific, Waltham (USA)
Hydrochloric acid (HCl)	Carl Roth GmbH, Karlsruhe (Germany)
L-Glutamine (200 mM)	Sigma-Aldrich Corp., St Louis (USA)
Laminin	Sigma-Aldrich Corp., St Louis (USA)
Low Melting Point Agarose	Invitrogen
Magnesium chloride ($MgCl_2$)	Sigma-Aldrich Corp., St Louis (USA)
M-CSF	Peprotech, Rocky Hill (USA)
Minimum Essential Medium (MEM)	Thermo Fisher Scientific, Waltham (USA)

NaCl solution 0.9 %	B. Braun AG, Melsungen (Germany)
N-Acetyl-D-Glucosamine (GlcNAc)	Sigma-Aldrich Corp., St Louis (USA)
Nogo-A rat FC	R&D Systems, Inc., Minneapolis (USA)
Nonidet P40	Applichem
Normal goat serum (NGS)	Vector Laboratories, Burlingame (USA)
Paraformaldehyde (PFA)	Carl Roth GmbH, Karlsruhe (Germany)
Pepstatin	Sigma-Aldrich Corp., St Louis (USA)
Penicillin / Streptomycin (P/S) (10,000 units penicillin and 10 mg streptomycin per mL)	Sigma-Aldrich Corp., St Louis (USA)
Percoll	Sigma-Aldrich Corp., St Louis (USA)
Poly-D-lysine hydrobromide	Sigma-Aldrich Corp., St Louis (USA)
Poly-L-ornithine	Sigma-Aldrich Corp., St Louis (USA)
Potassium bicarbonate	Sigma-Aldrich Corp., St Louis (USA)
Propidium iodide (PI)	Sigma-Aldrich Corp., St Louis (USA)
RNase AWAY	Molecular BioProducts
RNAse inhibitor	Clontech, Mountain View (USA)
RPMI 1640	Life Technologies Corp., Grand Island (USA)
Saponin	Carl Roth GmbH & Co. KG, Karlsruhe (Germany)
Sodium-beta-glycerophosphat	Carl Roth GmbH & Co. KG, Karlsruhe (Germany)
Sodium bicarbonate ($NaHCO_3$)	Carl Roth GmbH & Co. KG, Karlsruhe (Germany)
Sodium fluoride (NaF)	Carl Roth GmbH, Karlsruhe (Germany)
Sodium orthovanadate (NaV)	Carl Roth GmbH, Karlsruhe (Germany)
Sodium Pyruvate	Carl Roth GmbH & Co. KG, Karlsruhe (Germany)
Tris-HCl	Sigma-Aldrich Corp., St Louis (USA)
Triton X-100	Sigma-Aldrich Corp., St Louis (USA)
Trypan blue	Sigma-Aldrich Corp., St Louis (USA)

Buffer	**Ingedients**
Anesthesia solution	20 mL 50mg/mL Ketamine
	2.5 mL 2% Rompun
	in 77.5 mL 0.9 % NaCl solution
FACS Buffer	0.5 % BSA
	in PBS
MACS Buffer	0.5 % BSA
	0.5 M EDTA
	in PBS
MEM (2x)	160,93 g MEM
	+ 0.35 g $NaHCO_3$

	+ 5 L Aqua dest.
5x Laemmli Buffer	250 mM Tris-HCl (pH 6.8)
	10% SDS
	30% Glycerol
	5% β-mercaptoethanol
	0.02% Bromophenol blue
Lysis Buffer	20 mM Tris-HCl
	150 mM NaCl
	5 mM EDTA
	Protease inhibitors
	1 µg/ml Pepstatin
	50 mM sodium fluoride
	1 mM sodium orthovanadate
	1 mM p-nitrophenyl phosphate
	Na-b-glycerophosphate
	10% glycerol
Paraformaldehyde (PFA) buffer 4 %	40 g Paraformaldehyde
	+ 1000 mL 0,1 M PBS buffer, pH 7.0 – 7.4
10x Running buffer	250 mM Tris
	1.92 M Glycine
	1% SDS
	adjust pH to around 8.3
Saponine Buffer	0.5 % Saponine
	0.5 % BSA
	in PBS
Stripping Buffer	6 M Guanidine hydrochloride
	0.2% Nonidet P-40
	20 mM Tris (pH 7.5)
	add 0.1 M (70 µl/10 ml) β-mercaptoethanol freshly before use
Transfer buffer	15% Methanol
	25 mM Tris
	192 mM Glycine
10x TBS	0.5 M Tris
	1.5 M NaCl
	adjust pH to 7.4
1x TBS-T	0.05% Tween-20 in 1x TBS
Immunoprecipitation buffer	20 mM Tris-HCL pH 7,5
	150 mM NaCl
	5mM EDTA
	1µg/ml pepstatin

Media	Ingedients
Cortex dissecting medium	10 mM Tris
	1x MEM
	0.18 g/ml 1 M dextrose
Cortex culture medium	2% B27
	2% horse serum
	0.5% PenStrep
	1x Glutamax in Neurobasal

2.1.2 Instruments

Instrument	Company
Autoclave Heraeus	Thermo Fisher Scientific, Waltham (USA)
Analog Vortex Mixer	VWR International GmbH, Darmstadt (Germany)
BD FACS Canto II	BD Bioscience, Franklin Lakes (USA)
Cell Counting Chamber Neubauer improved	Brand , Wertheim (Germany)
Cell Culture Incubator	Binder GmbH, Tuttlingen (Germany)
Cell Culture Microscope, bright field	Hund, Wetzlar (Germany)
Centrifuge Multifuge Heraeus XIR	Thermo Fisher Scientific, Waltham (USA)
Confocal Laser Scanning System SP8	Leica GmbH, Wetzlar (Germany)
Eppendorf Research Adjustable-volume Pipettes	Eppendorf GmbH, Wesseling-Berzdorf (Germany)
Fridges and Freezers	Liebherr, Bulle (Switzerland)
Freezer (Sanyo)	EWALD Innovationstechnik GmbH, Rodenberg (Germany)
Gamma irradiator Gammacell 2000	Mølsgaard Medical, Risø (Denmark)
Horizontal Laminar Flow Hood Heraguard	Thermo Fisher Scientific, Waltham (USA)
Magnetic Stand Ambion	Thermo Fisher Scientific, Waltham (USA)
McILWAIN tissue chopper	Campden Instruments LTD, Loughborough (England)

MidiMACS and QuadroMACS Separators	Miltenyi Biotec GmbH, Bergisch Gladbach (Germany)
Pipetus	Hirschmann Laborgeräte GmbH & Co.KG, Eberstadt (Germany)
Platform Shaker	Edmund Bühler GmbH, Hechingen (Germany)
Precellys	Peqlab GmbH, Erlangen (Germany)
Surgery Instruments	Fine Science Tools Inc., Heidelberg (Germany)
TC10™ automated cell counter	Bio-Rad Laboratories GmbH, München (Germany)
Thermal Cycler	Peqlab GmbH, Erlangen (Germany)
Vibratome Microm HM650V	Thermo Fisher Scientific, Waltham (USA)
Water bath Aqualine AL18	Lauda GmbH & CO. KG, Lauda-Königshofen (Germany)

2.1.3 Laboratory Supplies, Plastics and Glassware

Product	**Company**
Cell Counting Slides for TC10™/TC20™ Cell Counter, Dual-Chamber	Bio-Rad Laboratories GmbH, München (Germany)
Cell Culture Dish, polystyrene, Ø 60 mm + 100 mm	Greiner Bio-One GmbH, Frickenhausen (Germany)
Cell strainer, nylon mesh, 100 µm	BD Bioscience, Franklin Lakes (USA)
Centrifuge Tubes, polypropylene (PP), 15 mL + 50 mL	Greiner Bio-One GmbH, Frickenhausen (Germany)
Cling film	Carl Roth GmbH, Karlsruhe (Germany)
Eppendorf Tubes 1.5 mL + 2 mL	Eppendorf GmbH, Wesseling-Berzdorf (Germany)
Hypodermic Needle 20G + 27G	BD Microlance, Gateshead (UK)
Microscope glass slides	Thermo Fisher Scientific Inc., Waltham (USA)
Multiplate PCR Plates, 96 Wells, clear	Bio-Rad Laboratories GmbH, München (Germany)

Multiwell Plate, tissue-culture treated polystyrene, 24-well, 48-well, 96-well	BD Bioscience, Franklin Lakes (USA)
Pipette tips 10 µL, 200 µL, 1000 µL	VWR International GmbH, Darmstadt (Germany)
Filter pipette tips 10 µL, 200 µL, 1000 µL	Starlab, Hamburg (Germany)
Polystyrene Round Bottom Test Tubes 5 mL (FACS tubes)	BD Bioscience, Franklin Lakes (USA)
Scalpels	B. Braun AG, Melsungen (Deutschland)
Serological Pipettes, polystyrene, 5 mL + 10 mL + 25 mL	Greiner Bio-One GmbH, Frickenhausen (Germany)
Syringe, 1 mL + 2 mL + 30 mL	B. Braun AG, Melsungen (Deutschland)

2.1.6 Antibodies

Primary antibody	**Species**	**Company**	**Number**	**Application and dilution**
Anti-Actin, beta	Mouse	MP Biomedicals	691001	WB 1:10.000
Anti-Calmodulin	Rabbit	Abbexa	abx010483	WB 1:1000
Anti-Gap43	Rabbit	Abcam	ab7462	WB 1:1000
Anti-P-Gap43	Goat	Santa Cruz	17109	WB 1:750
Anti-GRB2	Rabbit	Santa Cruz	sc-255	WB 1:200
Anti-IL-13R alpha	Rabbit	Abcam	ab79277	WB 1:1000 ICC 1:200
Anti-IL-2R gamma	Rabbit	Abcam	ab180698	WB 1:1000 ICC 1:200
Anti-IL-4Ra (CD124)	Rat	BD Pharmingen	551853	ICC 1:50
Anti-IL-4Ra (CD124)	Rabbit	Bioss (BIOZOL)	bs-2458R	WB 1:1000 ICC 1:100
Anti-IL-4Ra (CD124)	Rabbit	Novus	NBP1-19727	WB 1:1000 ICC 1:50

Anti-IL-4Ra (CD124)	Rabbit	Abnova	PAB26977	WB 1:1000 ICC 1:100
Anti-IRS-1	Rabbit	Millipore	06-248	WB 1:1000
Anti-IRS-1	Mouse	Cell Signaling	3194	IP
Anti-P-IRS-1	Rabbit	abbexa	abx011015	WB 1:1000
Anti-MAPK p44/42	Rabbit	Cell Signaling	9102S	WB 1:500
Anti-pMAPK p44/42	Rabbit	Cell Signaling	4370S	WB 1:500
Anti-NeuN	Mouse			ICH 1:1000
Anti-PKCγ	Rabbit	Abcam	ab4145	WB 1:500
Anti-P-PKCγ	Rabbit	Bioss (Biozol)	bs-3729R	WB 1:500
Anti-Pi3K	Rabbit	Cell Signaling	4257	IP WB 1:1000
Anti-Pi3K	Rabbit	abbexa	abx215715	WB 1:200
Anti-SHC	Rabbit	MERCK	06-203	WB 1:1000
Anti-STAT6	Rabbit	Abcam	ab32520	WB 1:1000
Anti-pSTAT6	Rabbit	Abcam	ab125308	WB 1:1000
Anti-Tubulin, alpha	Mouse	Thermo Scientific	MMS-581-P1	WB 1:5000
Anti-Tubulin, beta 3	Mouse	Covance (Hiss Diagnostics)	MMS-435P	ICC 1:500

Secondary antibody	**Species**	**Company**	**Application and dilution**
Anti-Mouse IgG (H+L), Alexa Fluor® 488 conjugate	goat	Invitrogen	IHC, ICC: 1:500
Anti-Mouse IgG (H+L), Alexa Fluor® 568 conjugate	goat	Invitrogen	IHC, ICC: 1:500
Anti-Rabbit IgG (H+L), Alexa Fluor® 488 conjugate	goat	Invitrogen	IHC, ICC: 1:500

Anti-Rabbit IgG (H+L), Alexa Fluor® 568 conjugate	goat	Invitrogen	IHC, ICC: 1:500
Anti-Rabbit IgG (H+L), Alexa Fluor® 647 conjugate	goat	Invitrogen	IHC, ICC: 1:500
Anti-Rat IgG (H+L), Alexa Fluor® 488 conjugate	goat	Invitrogen	IHC, ICC: 1:500
Anti-Rat IgG (H+L), Alexa Fluor® 568 conjugate	goat	Invitrogen	IHC, ICC: 1:500
Anti-Goat IgG (H+L), Alexa Fluor® 488 conjugate	donkey	Invitrogen	IHC, ICC: 1:501
Anti-Rabbit IgG (H+L), Alexa Fluor® 568 conjugate	donkey	Invitrogen	IHC, ICC: 1:500
Anti-Rabbit IgG (H+L), Alexa Fluor® 647 conjugate	donkey	Invitrogen	IHC, ICC: 1:500
Anti-Mouse IgG (H+L), Alexa Fluor® 568 conjugate	donkey	Invitrogen	IHC, ICC: 1:500

2.1.7 Animals

Mice were housed under specifically pathogen free (SPF) conditions at the central animal facility of the University Medical Center of the Johannes Gutenberg University Mainz at a twelve-hour dark/light cycle with free access to food and water. Surgical procedures and sacrificing were performed by instructed persons certified by the Federation for Laboratory Animal Science Association (FELASA).

All animal experiments were approved by local authorities (Landesuntersuchungsamt Rheinland-Pfalz: G15-1-022) and conducted according to the German Animal Protection Law.

2.1.8 Software

Adobe Photoshop CS5

Olympus cellSens Dimension 1.6

Microsoft EndNote X7

FlowJo 10

FusionCapt Advanced Fx7 software

GraphPad Prism 6

ImageJ (Fiji) (http://imagej.nih.gov/ij/) with the following plugins:

NeuronJ (https://imagescience.org/meijering/software/neuronj/)

Image Studio Lite 4.0

Laica LAS-AF Lite

Microsoft Excel 2010

Microsoft Word 2010

Tecan i-control 3.7.3.0

2.2 Methods

2.2.1 Cell culture

Cell culture experiments were performed under laminar flow hoods under sterile conditions. All materials used for cell culturing were sterilized or disinfected with 70 % ethanol prior to use. All in cell culture produced waste was autoclaved at 121°C for 20 minutes at 1 bar pressure. Cells were cultured at 37°C with 5 % CO_2 and 95 % humidity in incubators.

2.2.2 Isolation and dissociation of murine cortical neurons

Adult pregnant mice were killed by cervical dislocation and embryos (E17-18) were obtained. The brains from each embryo were isolated and the cortices were transferred to HBSS. After washing, the cortices were incubated in trypsin-EDTA solution containing 1% DNase at 37°C for 30 min. Subsequently, the cortices were triturated with a fire-polished Pasteur pipette 20-30 times. Tissue pieces were separated from the cortex cells by centrifugation. 10^6 Cells were plated in 6-well plates coated with PDL (0,5 mg/ml in H_20) and laminin (1 µg/ml in neurobasal medium). Neurobasal medium was changed every 48h.

2.2.3 Viability assay

The viability of *in vitro* cultured cortical neurons was measured by assessing the nuclear morphology and the membrane integrity. Cell death was triggered by exposure to a toxic dose of 1 µM NMDA for 18 h at 37°C. Distinguishing between healthy, injured and dead cells the culture was stained with propidium iodide (PI 50 µg/ml) in culture medium for 20 min. Since PI also stains RNA, the cells were treated with RNase (100 Kunitz U/ml) for 20 min at 37°C. After fixation with 4% PFA the cells were stained with DAPI and Tubβ3, as described in 2.2.9. The PI signal was analyzed at 568 nm excitation and 590 nm emission. While the common nuclear marker DAPI enters all cells, PI only enters necrotic cells or those undergoing late apoptosis when membrane integrity is lost. The cells displaying nuclei without PI signal are healthy cells. Cells displaying nuclear fragmentation, chromatin condensation, or nuclear condensation in presence of PI undergo apoptosis (Cummings and Schnellmann 2004).

2.2.4 Preparation of cortical neuronal explants

Neonatal mice (P1-P3) were decapitated and the brains were carefully isolated and transferred to an embedding mold filled with 37°C warm low melting point agarose diluted in cortex dissecting medium. Using a vibratome (Thermo Scientific, Microm HM650V) filled with cortex dissecting medium cooled at 4°C, the embedded brains were cut in coronal sections of 250 µm thickness. The brain sections ranging from Bregma 0 to -1,5 - comprising the motor cortex - were collected. The areas containing layer V of the motor cortex were dissected using micro scissors and divided in 4 equal explants that were plated on coverslips.

2.2.5 Cortex growth assay

Prepared neonatal cortex layer V explants as described above were cultured on glass 14 mm coverslips in 16 mm wells (4-well plates) coated with PDL (0,5 mg/ml in H_20) and Laminin (1 µg/ml in neurobasal medium) in DRG medium. Medium was exchanged with new IL-4 (50 ng/ml) every 24h. Explants were treated for 3 consecutive days with IL-4 (50 ng/ml) and PBS. Every 24h, the neurite outgrowth was recorded using a microscope equipped with a

cellSense camera. The neurite length was assessed using Adobe Photoshop by measuring the distance of the 40 longest axons, corrected for the initial growth after 24h.

For Nogo experiments the wells were coated first with nitrocellulose dissolved in methanol followed by Nogo-A (5 µg/ml) for 1h at 37°C (Snow, Lemmon et al. 1990, Wright, El Masri et al. 2007). After washing with PBS, the wells were coated with PDL (0,5 mg/ml in H_20) for another hour at 37°C. Cortex explants were plated and cultures were imaged after 24 and 48h.

2.2.6 Immunocytochemistry (ICC)

Glass coverslips with cells/explants were washed twice with PBS and placed in a staining chamber. For permeabilization and blocking of potential unspecific antibody binding sites the explants were incubated with ICC blocking solution (5% serum, 1% BSA in PBS-Tx) for 1 h at RT. Primary antibodies were diluted in ICC blocking solution and incubated on the coverslips over night at 4°C. Subsequently the coverslips were washed 3 times with PBS and incubated with the secondary antibodies diluted in ICC blocking solution for 1-2 h at RT. The coverslips were washed with PBS and mounted upside down on glass slides with aqueous mounting medium (VectaMount AQ). After a 24h curing phase the slides were stored at 4°C.

2.2.7 Immunohistochemistry (IHC)

For immunohistochemical analysis, the tissue was fixed by PFA perfusion. The mice were anesthetized by intraperitoneal injection of 1 ml anesthesia solution. By monitoring the tail and toe reflexes, the mouse sedation was assessed. After complete absence of the tail and toe reflexes the mice were fixed on cork tiles and access to the heart was gained by removal of the ribcage. After opening of the right atrium, 20 ml PBS was slowly injected into the left ventricle of the heart. Subsequently, 20 ml 4% PFA was slowly injected for tissue fixation. Target tissues were dissected and post-fixed in 4% PFA for 24h. After washing with PBS, the tissue was transferred to 30% sucrose for cryo-preservation. The tissue was then snap-frozen in embedding medium (Tissue-Tek O.C.T. Compound) and stored at -80°C. The tissue blocks were sectioned with a cryostat to a thickness of 10 µm; sections were mounted on glass slides and stored at -20°C until staining.

Tissue sections were dried on the slides and permeabillized with 0.2% PBS-Tx for 10 min. After washing with PBS for 5 min, the slides were incubated with 50 mM NH_4Cl for 10 min to demask antigens. For blocking of potential unspecific antibody binding sites, the explants were incubated with blocking solution (5% serum, 1% BSA in PBS-T) for 1 h at RT. Tissue sections were incubated over night at 4°C with the primary antibodies diluted in blocking solution. After another washing step with PBS, the secondary antibodies are applied with blocking solution for 1-2 h. Next the slides were coverslipped with FluorSafe Reagent.

2.2.8 Cell lysis and protein concentration analysis with Bradford

For protein analysis, 1-3x 10^6 dissociated cortical neurons were harvested from 6-well plates with plastic cell scrapers and transferred into 1.5 ml tubes with Precellys ceramic beads and lysed in 100 µl lysis buffer. Cell lysates were homogenized with the Precellys at 2x 5000 RPM and kept on ice. The protein concentration was measured with the Bradford protein assay, a spectroscopic analytical procedure based on Coomassie Blue G-250 which under acidic conditions is converted from red to blue. The absorbance shift at an excitation of 595 nm correlates with the protein concentration in the lysate. For calculation of the concentration a serial standard curve of seven different concentrations of BSA ranging from 0 to 20 µg/ml was included of triplicates of the standard curve and protein samples (diluted 1:50 in H_20) were pipetted in 96-well plates. The colorimetric reaction was started by the addition of 100 µl Bradford reagent and measured with the (Infinite M200 Pro, Tecan) after an incubation of 1 min.

2.2.9 SDS-Polyacrylamide-gel-electrophoresis (SDS Page)

In order to prepare the samples for gel electrophoresis they were mixed with Laemmli buffer and H_2O to achieve a concentration of 25 µg/ml at a total sample volume of 28 µl. The samples were heated at 95 °C for 10 min for denaturation of the tertiary structure and disulfide bonds of the proteins. Commercially available 10 % polyacrylamide gels (PeqLab) with 30 µl sample pockets were loaded with the protein samples and transferred into an electrophoresis cell

filled with running buffer. The proteins were separated under reducing conditions at 100-250 V, 2 mA for 40-90 min.

2.2.10 Western Blotting

After electrophoresis, the acrylamide gels were washed with transfer buffer and placed on Whatman filter paper soaked with transfer buffer. A nitrocellulose membrane was placed on top of the wet gel and topped with buffer-soaked filter paper. Depending on the targeted protein size semi-dry (below 60 kDa size) or wet (above 60 kDa size) blotting procedures were used. The semi-dry transfer was performed for 1,5 h at 29 V and 200 mA in the Trans-Blot Transfer Cell (BioRad). Wet transfers were performed for 1 h at 100 V and 2 mA in a Criterion Blotter (BioRad).

After the transfer, potential unspecific antibody binding sites were blocked with 1x RotiBlock solution for 1 h. Subsequently, the membranes were washed in 1x TBS-T for 30 min on a shaker. The incubation of the primary antibody was performed overnight at 4 °C in 1x RotiBlock solution. Next, the membranes were washed with 1x TBS-T for 30 min and incubated with the corresponding fluorescent secondary antibody (LiCor). Signal detection was performed with the LiCor Odyssey scanner.

For Western Blot detection of phosphorylation changes, primary antibodies detecting the phospho-antigens were stripped off the membranes after scanning for the first antibody signals. To achieve this, the membranes were incubated in stripping buffer twice for 5 min at RT. After stripping the membranes were washed in PBST for 10 min. Washing was repeated until no odors of the stripping buffer were detectable by scent. After washing, the membranes were again blocked with 1x RotiBlock solution for 1 h and subsequently incubated with the non-phosphorylated primary antibody diluted in 1x RotiBlock for 24h at 4°C. The procedures for secondary antibody incubation and fluorescence signal scanning were the same as for the phosphorylated antibody.

2.2.11 Co-Immunoprecipitation (Co-IP)

Neonatal cortical neuron cells were cultured for 6 d and harvested by scraping with ice-cold lysis buffer (see cortical neuron culture). The IP was performed using Protein-A/G agarose beads and target-binding antibodies. Before IP, the agarose beads were pre-incubated with IP buffer. The cell lysate was cleared for 30 min with 50% agarose bead slurry to reduce non-specific binding. The antibody binding was performed by incubating the cell lysate with primary antibody and the agarose beads with gentle rocking overnight at 4 °C. The samples were precipitated and washed with IP buffer by centrifugation with descending speeds for 2 min (starting with 6000 g and ending with 3000 g). After precipitation the antigen-antibody complex was eluted from the beads by boiling in 2x concentrated loading buffer for 10 min at 90 °C under constant shaking. The samples were loaded onto precast 10% SDS gels (Bio-Rad) after a 2 min centrifugation at 3000 g. Electrophoresis, Western blotting and staining were performed as described above.

2.2.12 Statistics

All statistical analysis was performed with GraphPad Prism 6. Data are presented as standard error of the mean (SEM) unless stated otherwise. For the comparison of two groups, the paired Student's T test was performed. To compare multiple groups, the one-way ANOVA test with Tuckey posthoc analysis was performed.

3. Results

3.1 IL-4R subtypes on neurons

In order to understand the effects of IL-4 on axon regeneration, it is important to know which IL-4R types are present on neurons. Immunocytochemistry on murine dissociated cortical neurons revealed the expression of the IL-4Rα, the common γ and the IL-13Rα1 chain. Moreover, it could be shown that there was a co-localization of the IL-4Rα with the common γ chain, forming the IL-4R type I, as well as with the IL-13Rα chain, forming the IL-4R type II on neurons (Figure 7).

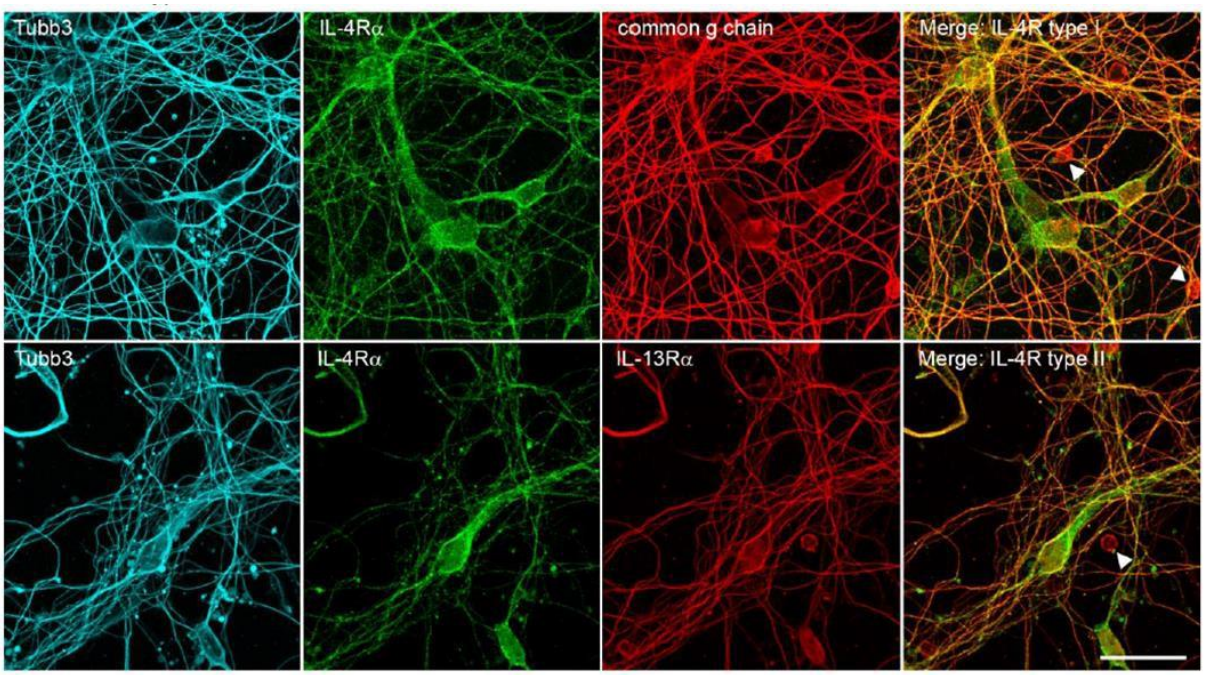

Figure 7: IL-4 receptor subtypes on neurons

Immunocytochemistry on cortical neurons marked by Tubb3 (left), co-stained for IL-4Rα (second), common γ chain (third, upper) or IL-13Rα1 (third, lower) and merged images (right). Small round, non-neuronal cells (arrowheads) are presumably oligodendrocytes, expressed IL-13Rα and γ chain, but not IL-4Rα. Scale bar = 25 µm (Adapted from Vogelaar, Mandal, Lerch *et al*. 2018)

3.2 IL-4 effects on neurite outgrowth *in vitro*

After the validation of the IL-4R subunits on cortical neuron cultures, the neuroprotective potential of the receptor activation by IL-4 was investigated. Here, a neuron viability assay was performed where cultures were treated with NMDA to induce apoptosis. After a 24h exposure to NMDA, the PBS-treated control neurons showed an 80 % incorporation of propidium iodide (PI) in the $DAPI^+$ nucleus. The neurons treated with IL-4 (50 ng/ml) only displayed a 20% incorporation of PI, indicating a protecting effect of IL-4 against damage due to excitotoxicity (Figure 8).

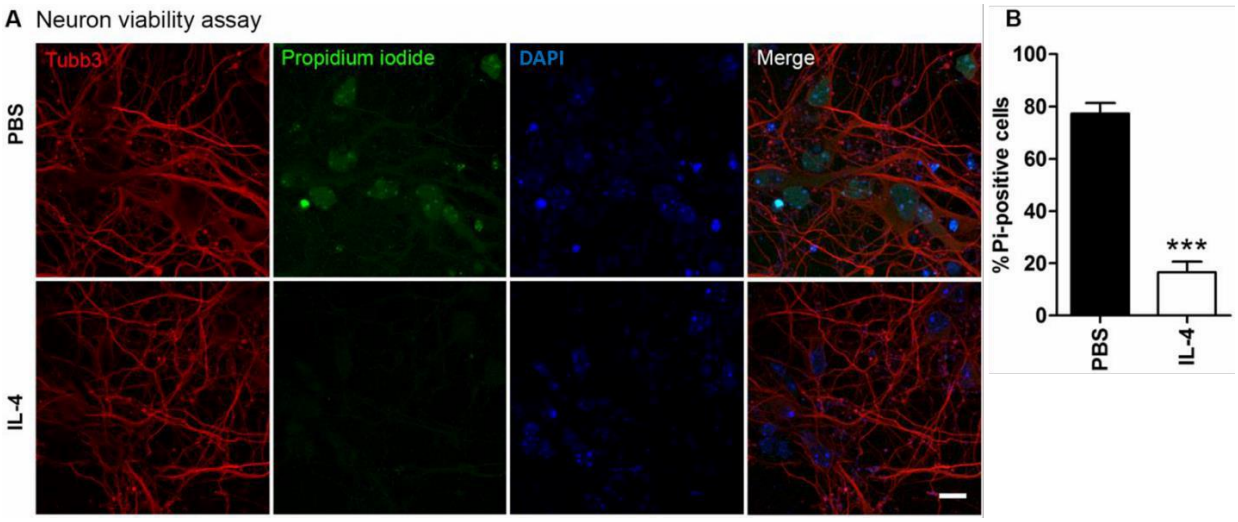

Figure 8: Neuron viability assay

Dissociated cortical neurons incubated with 1 µM NMDA and simultaneous treatment with PBS or IL-4 (50 ng/ml) respectively for 24h followed by incubation with propidium iodide (Pi). **A** Immunocytochemistry stainings with Tubb3 (red), Pi (green) and DAPI (blue). **B** IL-4-treated neurons displayed significantly less positive Pi signals compared to very strong Pi positive signals in the PBS control group. Statistic: Unpaired t-test *p < 0.05, ** p < 0.01, *** p < 0.001 Scale bar = 10 µm. (Adapted from Vogelaar, Mandal, Lerch *et al*. 2018)

To specifically model corticospinal tract (CST) axons *in vitro*, a novel cortical explant culture was developed (Liu, Shi et al. 2005). Layer V of the motor cortex, containing the CST projection neurons, was specifically dissected from neonatal brains and cultured on PDL/laminin-coated plates to provide optimal conditions for axon growth. Compared to the dissociated neurons,

the cortex tissue explants grew long axons and only showed minor cell migration from the explant within the first 3 days *in vitro*. Furthermore, the explants displayed robust outgrowth of axons from 1 day for up to 2 weeks in culture, reaching a total radius of 2 mm around the explant. These explant cultures allowed the quantitative and qualitative analysis of treatment effects on CST axons (Figure 9 A).

To score treatment effects of IL-4 (50 ng/ml), IL-13 (50 ng/ml) or PBS vehicle (equal volumes) explants were allowed to grow for the first 24h without treatment, in order to assess baseline outgrowth and select explants with similar starting points. Then, treatments were applied for 24h and refreshed during the next day. Light microscopic images were taken daily (see Fig. 9A time line) and the 40 longest axons were measured. When explants grew more than 40 axons, which was usually the case at d1 and d2, 10 axons in each cardinal direction were analyzed. To optimize the model for the quantification of treatment effects, IGF-1 was used as a positive control (Figure 9E). IGF-1-treated explants displayed a significant increase in neurite outgrowth compared to the control PBS (Figure 9E). Axons treated with PBS displayed a 2-fold growth increase after 48h, whereas the IL-4-treated (50 ng/ml) explants showed a 4-fold increase in outgrowth. Similarly, after a total period of 72h, IL-4-treated axons grew two times faster than the PBS control group (Figure 9 B). This effect was completely abolished in cultures originating from CamKIIα Cre-driven IL-4Rα KO mice (Figure 9 C). Since IL-13 and IL-4 are competitive ligands for the IL-4R type II (Figure 4), the direct effects of IL-13 on cortex layer V explants were assessed. However, IL-13-treated (50 ng/ml) cortical axons did not show a difference in outgrowth compared to PBS at any time point (Figure 9 D).

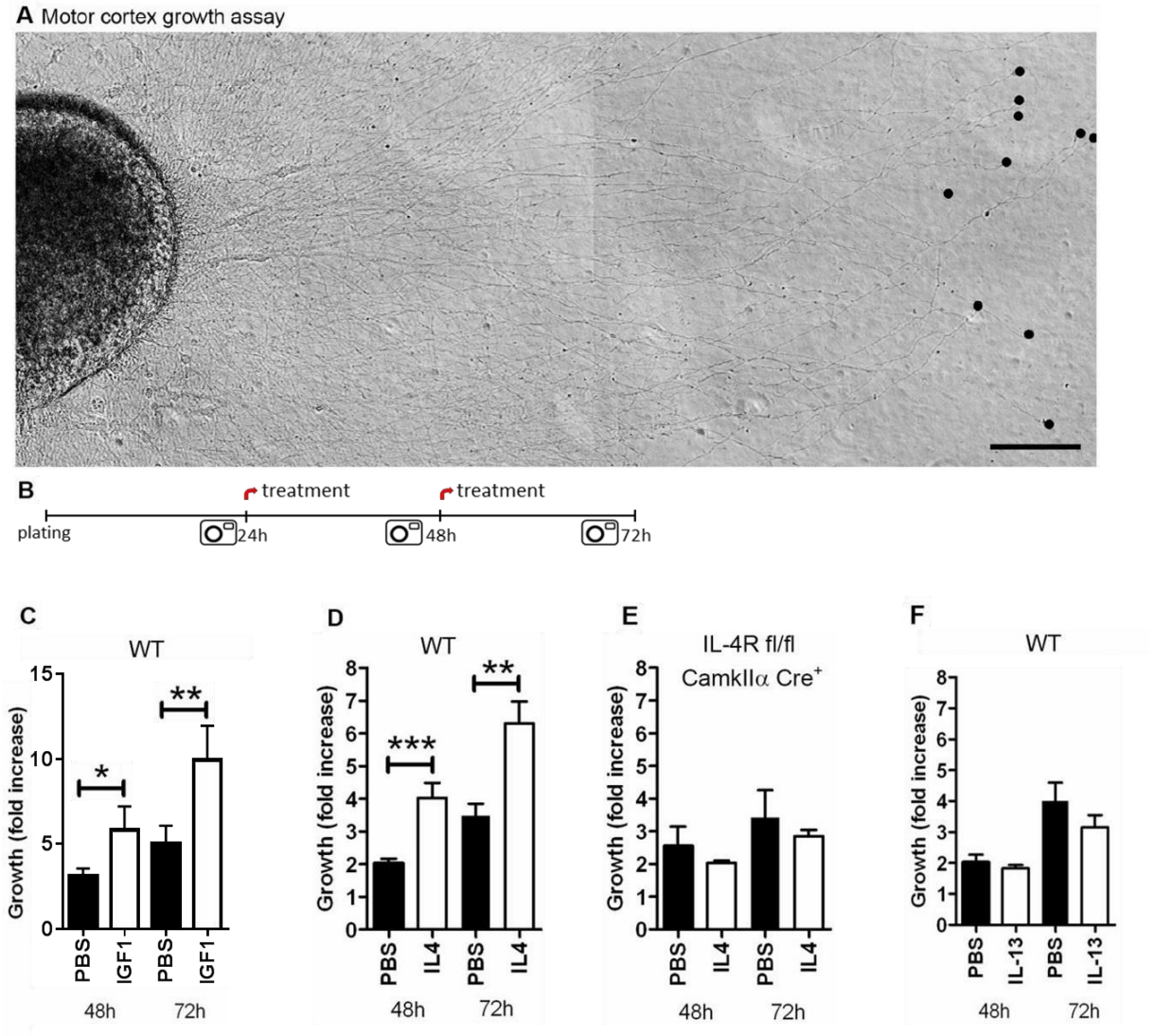

Figure 9: IL-4 acts beneficially on neurite outgrowth

A Motor cortex layer V explants grew long axons in vitro after 2-3 days *in vitro* (div). The 10 longest axons are marked with black dots. Scale bar = 100 µm. **B** Time line of growth assay with daily imaging (camera symbol) and treatment at 24 h and 48 h. **C** IGF-1 (50 ng/ml) treated explants grow significant longer neurites compared to IL-4 and PBS treated explants. **D** Quantification of the treatment effects on axon outgrowth after 48 h and 72 h, calculated as fold increase compared to 24 h baseline growth. **E** In cortical explant cultures of IL-4Rfl/fl CamKIIα Cre mice the effect of the IL-4 treatment on axonal outgrowth abolished. **F** Treatment with IL-13 did not show an effect on axonal outgrowth in cortex explant cultures. *p < 0.05, ** p < 0.01, *** p < 0.001 (Adapted from Vogelaar, Mandal, Lerch *et al*. 2018)

The observed IL-4-induced axon growth *in vitro,* led to the investigation of IL-4 treatment effects on axonal outgrowth under inhibitory conditions. The intact CNS disposes of

mechanisms that inhibit axonal growth and neurite sprouting to prevent aberrant target innervation (Chew, Fawcett et al. 2012). This needs to be overcome in order to promote axon sprouting in case of an injury. Here, Nogo-A (5 µg/ml) was chosen as an inhibitory model for axon growth in our outgrowth assay. Culture plates were coated with Nogo-A before plating of the explants. The axon growth was assessed after 24 h and 48 h of culture. PBS-treated control cortex layer V explants showed hardly any axonal growth after 24h (Figure 10 A), whereas the IL-4-treated explants showed a significantly higher number of axons on the inhibitory coating (Figure 10 B). After 48h, the axon numbers on the IL-4-treated group was even higher, indicating a stimulating effect of IL-4 on the ability of CST axons to overcome inhibition (Figure 10 C).

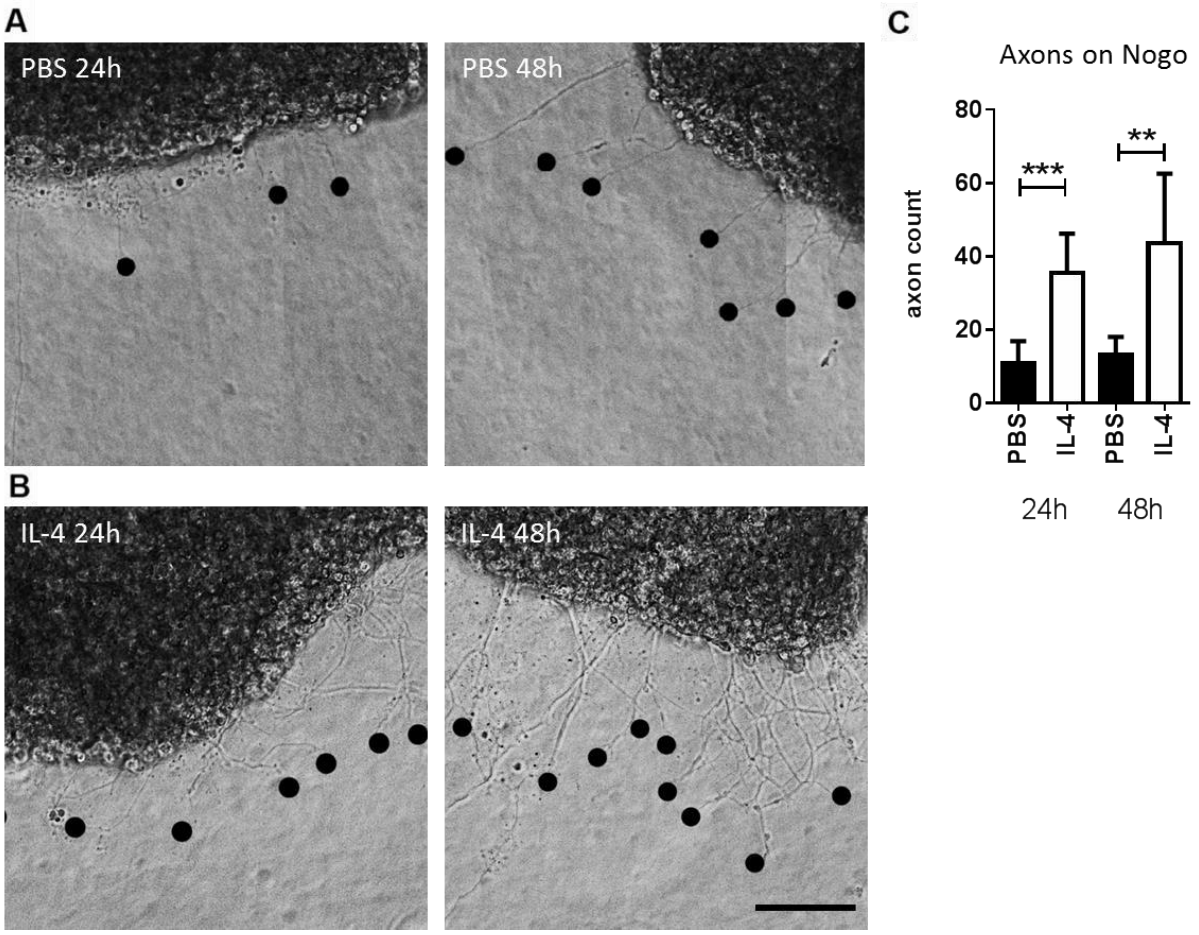

Figure 10: Overcome of growth inhibition by Nogo-A

Cortical layer V explants cultured on Nogo-A. **A** PBS-treated control explants displayed very little axon growth within 24 and 48h. **B** Treatment with IL-4 (50 ng/ml) resulted in a significant increase in axon numbers compared to the PBS control group at both time points. Statistics: Unpaired t-test; *** $p < 0.001$. Scale bar = 50 µm

3.3 Neuronal IL-4R signaling pathways

To date, the IL-4R signaling pathway is exclusively known in immune cells, like T helper cells, B cells, NK cells, mast cells and basophils (Nelms, Keegan et al. 1999). Previous work suggested that IL-4 worked indirectly on neurons by potentiating neurotrophin signaling (Walsh et al. 2015). However, it remained unclear if any direct neuronal IL-4R signaling cascades exist. Here, a neuronal IL-4R signaling pathway leading to cytoskeletal remodeling could be unraveled.

3.3.1 Co-localization of IL-4R and docking proteins

The expression of the IL-4R type I and II in dissociated neuron cultures was shown above by immunocytochemistry. Consequently, the IL-4-induced binding of docking proteins to the IL-4R was assessed using co-immunoprecipitation (co-IP) methodology on IL-4-treated homogenates of dissociated cortical neurons. By coupling the IL-4Rα complex to agarose beads, which were then incubated with the neuron homogenates, the resulting immunoprecipitated proteins were analyzed by Western blotting. Both the SH2 domain-containing adapter protein (Shc) and the insulin receptor substrate 1 (IRS1) were detected in the IL-4R-bound output, indicating that these proteins are present in the receptor complex (Figure 11 A). In a second co-IP experiment the recruitment of PI3K to the IL-4R-IRS1 complex was quantified. Compared to the PBS control group, significantly more PI3K was found to be bound to the receptor when the neurons were treated for 30 min with IL-4 (Figure 11 B).

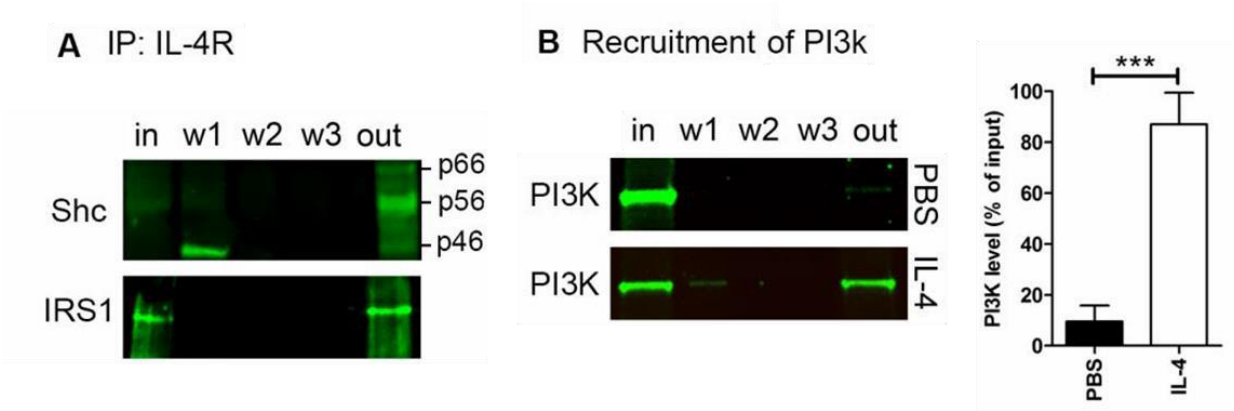

Figure 11: Co-IPs of IL-4Rα with docking and signaling proteins

A Co-IP showed binding of the docking proteins Shc and IRS1 to the IL-4R in cortical cell homogenate output (out). Samples of the washing steps (w1-3) showed removal of the unbound target proteins, compared to the cell input (in). **B** PI3K was increased in the IL-4R–IRS1 complex after IL-4 treatment, compared to PBS-treated homogenates. (Adapted from Vogelaar, Mandal, Lerch *et al*. 2018)

3.3.2 Phosphorylation cascade upon IL-4 stimulation

In order to understand how the signaling cascade initiated upon IL-4R activation with IL-4 progresses intracellularly in neuronal cells, homogenates of dissociated cortical neuronal cultures were analyzed. The cortical neurons were treated with IL-4 (50 ng/ml) or equal volumes of PBS for 10 min prior to being harvested and lysed. Western blot analysis with antibodies against the target proteins and their corresponding phosphorylated epitopes was performed for potential pathway proteins. As the first player in the cascade, IRS1 phosphorylation was significantly increased (Figure 12 A-B). PI3K, being recruited to the IL-4R upon IL-4 stimulation (see Figure 11) is not regulated by phosphorylation, therefore, the downstream signaling molecule PKC was focused on, (see also Figure 6). More specifically - in view of the above-described outgrowth data – we focused on the CST marker PKCγ. Indeed, PKCγ phosphorylation was significantly increased in IL-4-treated cortical neurons (Figure 12 A-B). Furthermore, the known PKC target GAP-43 displayed a significant increase in phosphorylation (Figure 12 **Error! Reference source not found.**A-B). On the other hand, the u pregulation in phosphorylation after IL-4 treatment of all signaling molecules in cortical neurons isolated from IL-4R KO CamKIIα Cre^{+} mice was partially abolished Figure 12 C). Application of IL-13 did not result in phosphorylation of IRS-1, PKCγ or GAP-43 (Figure 12 D).

The IL-4-mediated release of CaM from GAP-43 marks an essential step in the initiation of actin modulating pathways. Co-IPs were performed to prove that this takes place downstream of IL-4 signaling. A significant decrease in CaM signal could be shown in homogenates of IL-4-treated neurons after Co-IP with GAP-43 antibody (Figure 12 E-F).

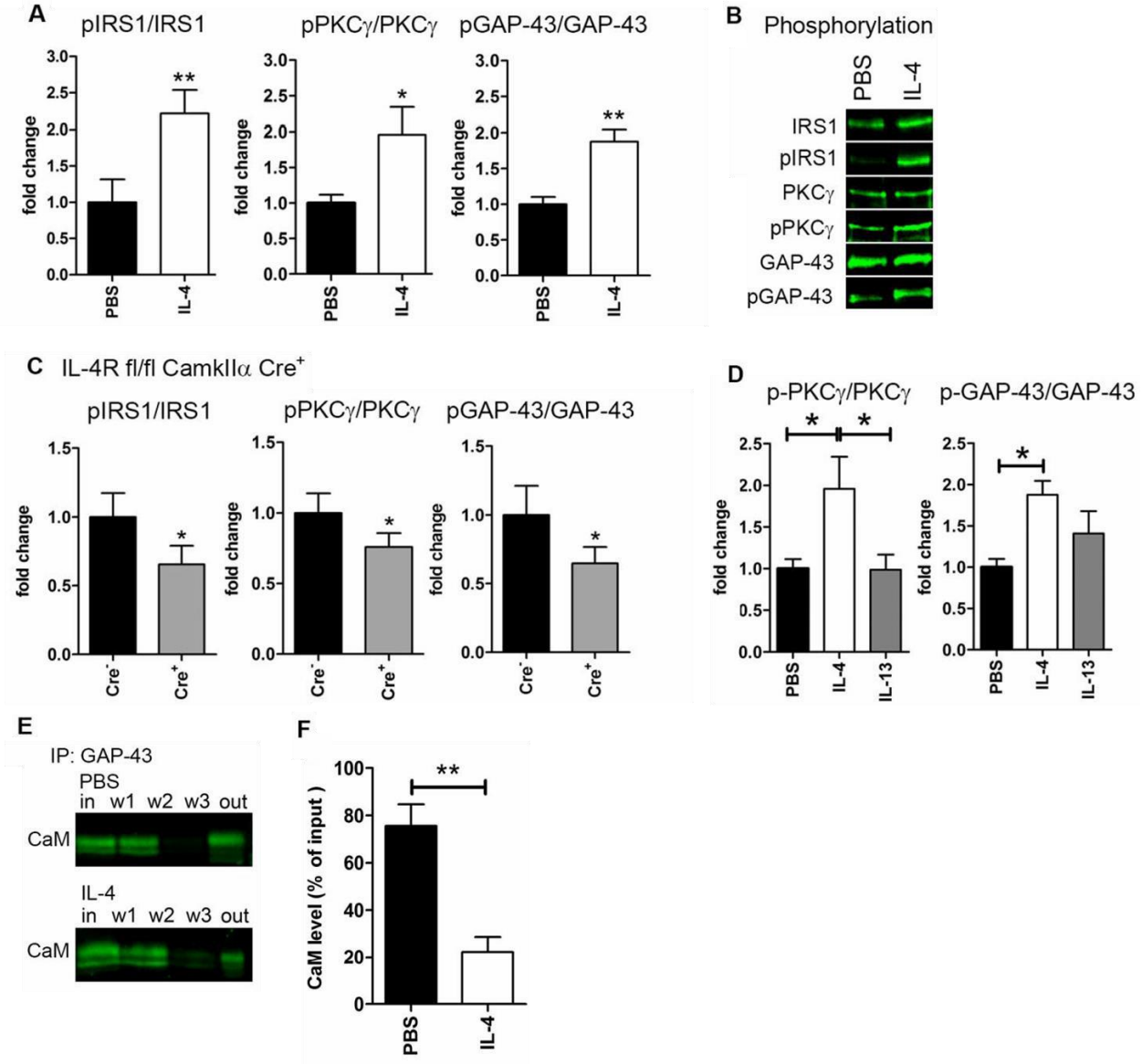

Figure 12: Phosphorylation of putative components of the IL-4R signaling cascade upon IL-4 stimulation in cortical neurons

A Quantification of Western Blots (**B**) for phosphorylated protein and total protein for IRS1 (n = 3), PKCγ (n = 9-11) and GAP-43 (n = 6-7) showing increased phosphorylation in response to IL-4. **C** Cortical neurons from IL-4R fl/fl CamKIIα Cre mice showed a significantly reduced phosphorylation of IRS1, PKCγ and GAP-43 in response to IL-4. **D** Phosphorylation on PKCγ and GAP-43 did not change after incubation with IL-13 (50 ng/ml) in comparison

to PBS-treated controls. **E**. Co-IP with GAP-43 and staining for CaM showed reduced binding in IL-4-treated homogenates compared to PBS control. **F** Quantification of CaM release upon IL-4 treatment. Statistics: unpaired t-test or one-way ANOVA with Tuckey's multiple comparison test for phosphorylation assays. *p < 0.05, ** p < 0.01, *** p < 0.001 (adapted from Vogelaar, Mandal, Lerch *et al*. 2018)

In addition to Western blot analysis on homogenates of dissociated cortical neurons, ICC stainings were performed to show the distribution of GAP-43 and PKCγ and the corresponding phosphorylated proteins. The neuronal marker tubulin β3 (Tubb3) was used to mark neurons and their axons (Figure 13 A). A consistent and homogeneous distribution of GAP-43 and PKCγ signal in cortical neurons was observed (Figure 13 B-C). Phosphorylated PKCγ was highly abundant in cell bodies and distributed in a sparse punctuate pattern in neurites (Figure 14B). Similarly, phosphorylated GAP-43 was enriched in the neuronal cell body as compared to the processes (Figure 13 C). This indicates that the proteins were only activated in specific cellular compartments.

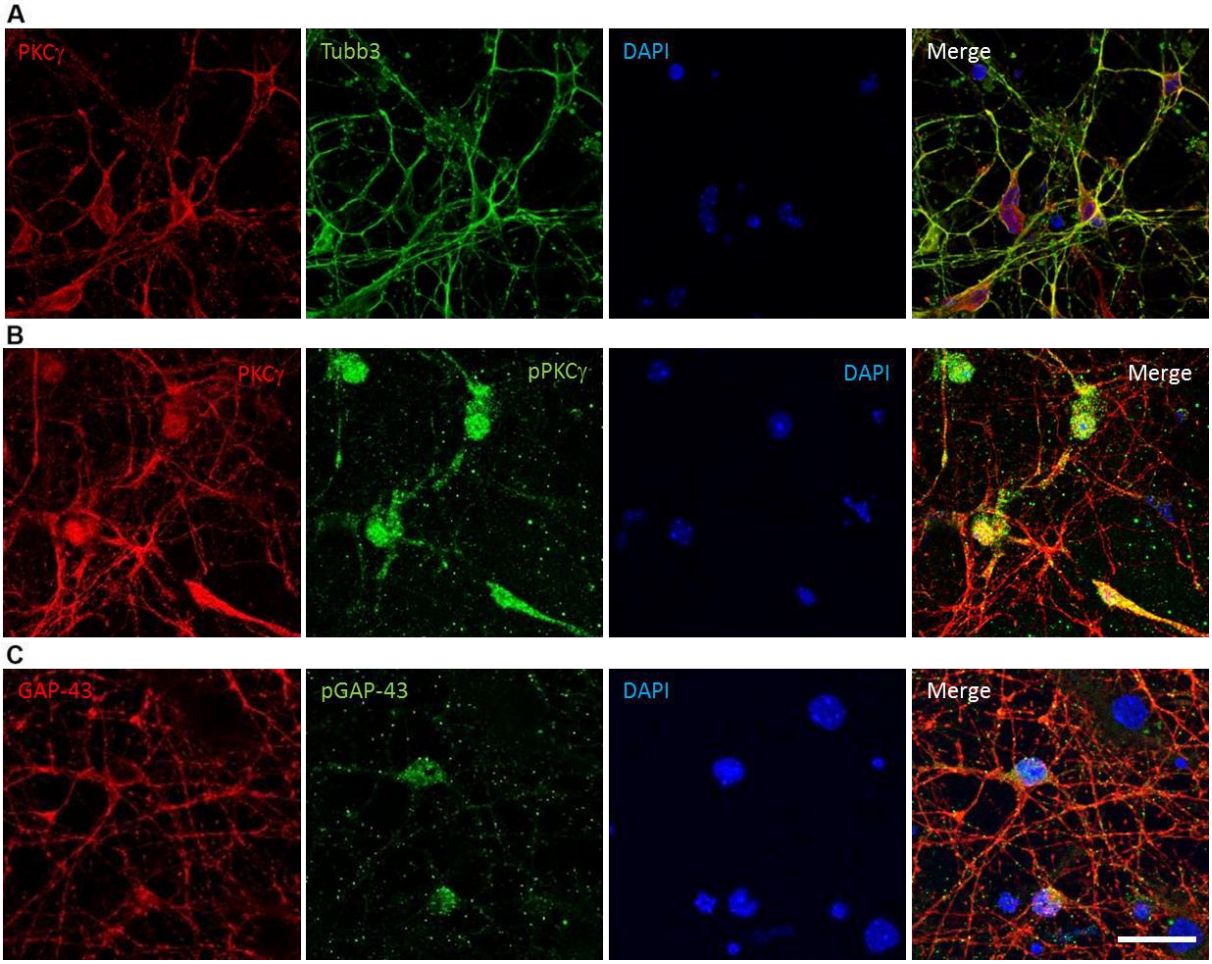

Figure 13: Immunocytochemistry of phosphorylated and un-phosphorylated GAP-43 and PKCγ

A ICC on dissociated embryonal cortex cultures for PKCγ (red) and neuronal marker Tubb3 (green). **B** ICC for PKCγ (red) staining neurites and cell bodies and corresponding staining for pPKCγ (green) predominantly in neuronal cell bodies. **C** Stainings for GAP-43 (red) and pGAP-43 (green) displaying a similar signal distribution as pPKCγ/PKCγ. Scale bar = 20 µm.

3.3.3 IL-4R signaling through PKC and GAP-43 play a role in actin cytoskeleton remodeling

Our *in vivo* experiments in the EAE model (Vogelaar, Lerch et al. 2018) suggest that IL-4 is able to repair axonal swellings (work performed by Shibajee Mandal). Since PKC and GAP-43 are both known to be involved in cytoskeletal remodeling (Oestreicher et al, 1997), it was investigated whether the actin cytoskeleton is altered after IL-4 treatment. Phalloidin stainings were used to mark filamentous actin (F-actin) in dissociated cortical neuron cultures. After incubation with IL-4 (50 ng/ml) for 30 min, the cells displayed a shift in F-actin signal. The

PBS-treated control neurons showed patch-like clusters of F-actin in the cell bodies and neurites (Figure 14 **Error! Reference source not found.**A), while in IL-4-treated cultures strong f ilamentous patterns were observed (Figure 14 B). Quantification of the phalloidin-positive filaments showed a significant increase in F-actin signal length in IL-4-treated neurons compared to all other treatments (Figure 14 E). The activation of PI3K leads to the opening of Ca^{2+} channels in neurons (Nicholson-Fish, Cousin et al. 2016), which is known to activate PKC (Freeley, Kelleher et al. 2011). To investigate whether PKC activation is essential for actin remodeling in response to IL-4, the PKC inhibitor bisindolylmaleimide I (Bis1) was used. This compound occupies the ATP binding domains of classic PKCs (α, βI, βII, γ) with a very high affinity (IC_{50}=10-20 nM) thus inhibiting their functions (Freeley, Kelleher et al. 2011). Concurrent treatment of Bis1 abolished the IL-4 effect on F-actin in cortical neuron cultures (Figure 14 C, E) and on axonal outgrowth (Figure 15F). Application of BAPTA-AM, a Ca^{2+} chelator, also abrogated the IL-4 effects in culture (Figure 14 D-E).

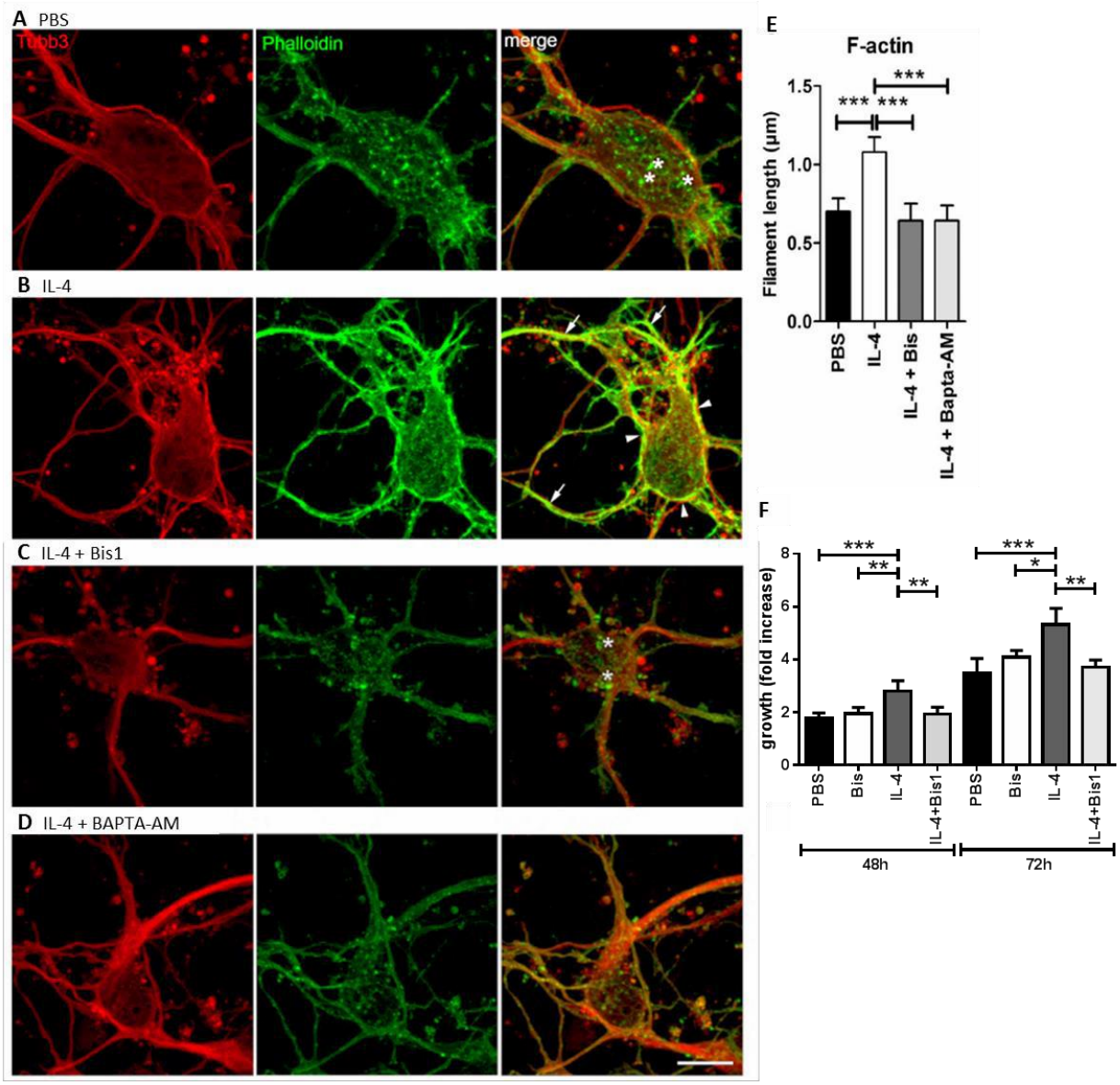

Figure 14: Cytoskeletal remodeling

A-D Immunocytochemistry for Tubb3 (red, left) and Phalloidin (green, middle), merged (right). **A** PBS-treated neurons displayed patchy clusters of F-actin (asterisks). **B** Treatment with IL-4 (30 min, 50 ng/ml) showed a significant change in F-actin signal in neurites (arrows) and a shift towards the cell body surface (arrowheads). **C** Co-treatment of IL-4 with Bis1 abolished this effect, in the same way as the combined treatment with **D** Ca^{2+} chelator BAPTA-AM. **E** Quantification of actin filament length. **F**. Quantification of the treatment effects on axon outgrowth after 48h and 72h compared to 24h baseline growth. Co-treatment with IL-4 (50 ng/ml) and Bis1 (100 nM) abolishes the IL-4 effect on neurite outgrowth whereas Bis1 alone has no effect on neurite outgrowth. Scale bar = 10 µm. Unpaired t-test; one-way ANOVA with Tuckey's multiple comparison test; * $p < 0.05$, ** $p < 0.01$, *** $p < 0.001$ (Adapted from Vogelaar, Mandal, Lerch *et al*. 2018)

3.4 IL-4 effects on neurite outgrowth *in vivo*

To investigate whether the above-described signaling pathway, leading to axon growth, really takes place *in vivo*, the sprouting of CST neurons in EAE mice was traced. For this purpose, the anterograde tracer rhodamine-conjugated dextran was injected into the motor cortex of Bl6 mice seven days prior to EAE induction. IL-4 treatment (1 µg/mouse, applied via lumbar intrathecal injection) was started 5d after peak (Figure 16 A, grey bar) and after 10 d the animals were perfused and the CST tissue was processed for imaging (EAE induction, surgery and animal care were performed by Shibajee Mandal). Analysis of the traced CST revealed significant sprouting of axons from the CST into the grey matter of IL-4-treated animals compared to the PBS-treated controls (Figure 15 B). Comparison of the tracing density showed no significant difference in tracing efficiency between the groups (Figure 15 C). Finally, to show the existence of this IL-4R signaling pathway *in vivo*, immunohistochemistry on EAE animals was performed on spinal cord sections from the tracing experiment. Here, IL-4 treatment resulted in an increase of pIRS1-positive axons compared to PBS control in the CST and also in the dorsal columns (DC) (Figure 15 D-E).

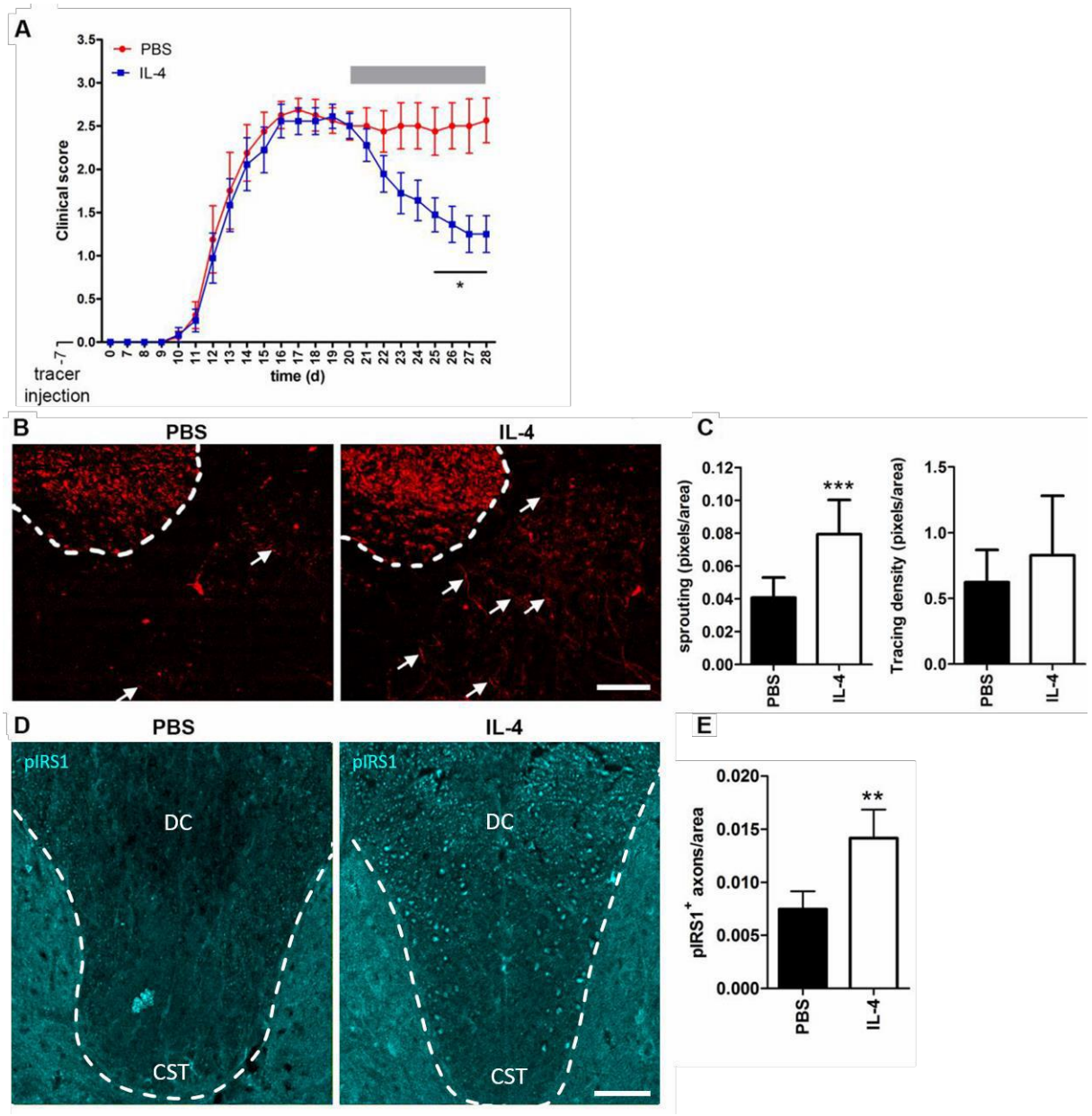

Figure 15: Neuron tracing of the dorsal CST

A Injection of anterograde tracer 7 days before EAE induction and treatment with IL-4 or PBS during chronic disease phase (grey bar) of Bl6 EAE. Mice showed typical disease course (clinical score) and response to IL-4 treatment (analyzed by S. Mandal). **B** IL-4-treated EAE mice displayed increased sprouting of axons reaching from the dorsal CST (dashed line) into the grey matter (arrows). Scale bar = 50 µm. **C** Quantification of axonal sprouting and tracing signal density (n = 4 animals, 3 sections per animal). **D** CST and DC immunohistochemistry for pIRS1 (cyan) on spinal cord tissue from IL-4- and PBS-treated EAE mice. Scale bar = 50 µm. **F** Quantification of pIRS1-positive axons after correction for the size of the analyzed area (n = 5). Statistics: unpaired t-test *p < 0.05, ** p < 0.01, *** p < 0.001 (Adapted from Vogelaar, Mandal, Lerch *et al*. 2018)

Altogether, this points towards an IL-4-mediated signaling through IL-4R via the IRS-PI3K-PKC signaling pathway in cortical neurons. Moreover, the data suggest that PKC, GAP-43 and CaM – main regulators of cytoskeletal remodeling - are responsible for the IL-4 effects on F-actin. The here presented signaling cascade is likely to mediate axon outgrowth and sprouting, therewith resulting in a partial recovery of clinical symptoms of EAE mice.

4. Discussion

In this thesis, it was aimed to unravel the neuronal IL-4R signaling pathway and to shed more light on the direct effects on cortical neurons that project long axon tracts in the spinal cord, both affected by neuroinflammation (DeLuca, Ebers et al. 2004). To this purpose, we developed functional assays and correlated these with biochemical analysis of key signaling molecules.

To date, the strategies of MS treatments concentrate on the alteration of the immune system, whereas the axon compartment has not been adequately targeted (Franklin, ffrench-Constant et al. 2012, Zipp, Gold et al. 2013, Larochelle, Uphaus et al. 2016). Common treatments involve the modulation of dendritic and T cell properties or the impairment of the T cell release from the lymphatic organs (Deshmukh, Tardif et al. 2013, Jolivel, Luessi et al. 2013, Kraus, Luessi et al. 2014). Modern histopathology and imaging techniques revealed that already in the earliest stages of the disease significant damage in neuronal structures occurs. Neuronal pathology accumulates as the disease progresses leading to accumulation of axonal loss and disability (Zipp and Aktas 2006).

Previous studies showed evidence that T lymphocytes and their cytokines not only do harm to neurons, but in particular T helper 2 (T_H2) cells can have beneficial effects in experimental neurotrauma and experimental autoimmune encephalomyelitis (EAE) (Payne, Dantanarayana et al. 2012, Walsh, Hendrix et al. 2015). In the CNS, IL-4-producing T_H2 cells display functions to restore the homeostasis of neurons and the surrounding cells (Ellwardt, Walsh et al. 2016). Moreover, we have shown that IL-4R is significantly expressed in tissue within MS lesions (Vogelaar, Mandal, Lerch et al. 2018). We now show that IL-4 has the potential to protect neurons against pathogenic stimuli and induces significant outgrowth of neurites *in vitro*. In addition to the enhanced outgrowth, we demonstrated that IL-4 treated neurons can overcome outgrowth inhibiting effects *in vitro* (Figure 10) and *in vivo* (Figure 15). These are crucial properties for the consideration of novel neuroregenerative strategies. To strengthen these findings, we were able to unravel a direct and fast IL-4R signaling pathway in neurons

which (Figure 12) directly induces actin remodeling processes in favor of cellular repair and outgrowth of axons (Figure 14).

4.1 Experimental limitations

In our recent paper in Science Translational Medicine, we demonstrated that IL-4 reverses clinical severity in EAE. We found that IL-4 significantly reduced axonal swelling in the CST and that IL-4-treated mice displayed near-normal walking (Vogelaar, Mandal, Lerch et al. 2018). In order to study the mechanisms of IL-4 signaling, the timing of treatment is essential to determine the phosphorylation of signaling molecules, which is an almost impossible task *in vivo*, because of unknown diffusion rates of IL-4 into the nervous tissue, difficulties of immunological stainings for signaling molecules (not necessarily available for optimization in untreated tissue), and dilution of the effects due to different cell types. Therefore, it is essential to develop *in vitro* assays that are more specific for the targeted neurons and that can be controlled in view of timing of treatment and analysis of the effects.

When working with cortical neuron cultures, the maturity of the cells is a major experimental limitation. In this thesis, cortices for dissociated neuron cultures were exclusively taken from E18 mouse embryos, and neurons were allowed to maturate in culture for at least 7 d. These cultures are the best option to study phosphorylation, because they contain both cell bodies and neurites that are both likely to respond to IL-4. To study regeneration, however, dissociated cortical neurons are insufficient, because of their low viability and because these cultures, containing all neuron types from the complete cortex, are not specific for CST projecting neurons (Kriegstein and Dichter 1983, Lesuisse and Martin 2002).

Therefore, we established a novel model for *in vitro* CST regeneration by culturing explants dissected from motor cortex layer V. The dissected explants represented the hind limb region and contained the projection neurons that were able to grow long axons (Figure 9). These axons are positive for SMI-32 and PKCγ proving that they originated from CST neurons *in vitro* (Schnatz, Lerch et al, *in preparation*). The explants were isolated from P1-3, a developmental stage at which the neurons have already grown into the spinal cord (Gianinoa, Stein et al. 1999), so by dissecting the explants they are axotomized as opposed to developing. Finally,

after having obtained mechanistic and functional data in the *in vitro* assays, it is important to confirm some of these *in vivo*. In this thesis the mechanisms of neuronal IL-4R signaling *in vitro* were investigated. We also confirmed some of these mechanisms using the *in vivo* model.

4.2 Beneficial IL-4 effects on cell survival and outgrowth

Protection from excitotoxicity is a major issue in neurodegenerative diseases of the CNS like Alzheimer's disease, Parkinson's disease or (Maragakis and Rothstein 2006, Hajieva, Baeken et al. 2018), but it also may be involved in spinal cord injury, stroke or traumatic brain injury (Obrenovitch and Urenjak 1997, Park, Velumian et al. 2004, Lai, Zhang et al. 2014). Excitotoxicity is usually caused by an overload of glutamate binding to the NMDA receptor, causing a pathological elevation of Ca^{2+} influx into the cells. This leads to the activation of Ca^{2+}-dependent proteases, protein kinases and phosphatases that activate downstream pathways damaging the cytoskeleton, membranes and even the DNA (Manev, Favaron et al. 1989, Nicholls 2004, Norenberg and Rao 2007). With the viability assay, it was shown that IL-4 protected against NMDA-induced excitotoxic neuronal death, therefore, we concluded that IL-4 acts as a neuroprotective agent. We did not only observe neuronal protection but also found that IL-4 treatment increased neurite outgrowth. Here, the novel cortex outgrowth assay displayed significant increase in axonal outgrowth upon IL-4 treatment, indicative of regeneration and plasticity. Correspondingly, we observed increase axonal outgrowth on Nogo-A, one of the most potent myelin-derived growth inhibitory molecules (Mi, Hu et al. 2007, Giger, Hollis et al. 2010, Huebner, Kim et al. 2011). Upon contact of the oligodendrocyte-derived Nogo-A with the neuronal receptor Lingo-1, RhoA-GTP signal transduction in the growth cone activates the F-actin-depolymerizing enzyme cofilin (Pernet and Schwab 2012). The quick collapse of F-actin in the growth cone is triggered, causing the retraction of the cone (Nash, Pribiag et al. 2009). The ability to overcome inhibition by Nogo is a prerequisite for axon growth into normally non-permissive areas. These *in vitro* data correlate with the increased sprouting of CNS axons into the grey matter areas after IL-4 treatment *in vivo*.

Altogether, these functional assays show that IL-4 acts as a neuroprotective, growth-promoting agent that causes the axons to overcome inhibitory molecules. The combination of

these three mechanisms leads to the prevention of axon pathology and to axonal outgrowth and repair.

4.3 IL-4R signaling versus neurotrophin signaling in neurons

In previous studies of traumatic injury, we could show that IL-4 indirectly stimulated axon growth by enhancing neurotrophin signaling. Indeed, the signaling cascades of the neurotrophins NGF (nerve growth factor), BDNF (brain-derived neurotrophic factor), NT-3 (neurotrophin-3) and NT-4 (neurotrophin-4) (Lee and Chao 2001) share docking proteins IRS and GRB with the here shown IL-4R signaling pathway (Lee and Chao 2001). Moreover, it is commonly known that neurotrophin signaling trough the Trk receptor (tropomyosin receptor kinase) family activates PI3K/Akt and MAPK signaling resulting in increased cell survival, extending of growth cones and synaptic strength (Thoenen 1995, Gallo, Lefcort et al. 1997). In the peripheral nervous system (PNS), neurotrophins theoretically play a role in regenerative growth, however, there is a decrease in availability of neurotrophins in disrupted fibers accompanied with a decreased rate of retrograde transport (Raivich and Kreutzberg 1993, Leea, Shen et al. 1998). Although neurotrophins are upregulated in Schwann cells and satellite cells after injury, the Trk receptors (TrkA, -B and -C) in the PNS are not induced and TrkA is even downregulated (Vogelaar, Hoekman et al. 2003). Moreover, the phosphorylation of ERK after injury has been reported in Schwann cells, but not in neurons (Sheu, Kulhanek et al. 2000, Abe, Namikawa et al. 2001). These observations point to regeneration being regulated by mechanisms other than neurotrophic signaling. A role for neuroactive cytokines, rather than neurotrophins, in outgrowth of PNS neurons was proposed (Markus 2002). In the PNS, the neuroactive cytokine leukemia inhibitory factor (LIF) was shown to increase regeneration and LIF KO and IL-6 KO mice display decreased outgrowth of sensory neurons (William, Gardiner et al. 2001). In the CNS, however, IL-6 has rather detrimental pro-inflammatory properties, but here we postulate that IL-4 acts as a neuroactive cytokine in the CNS. This thesis supports that IL-4 induces a direct neuronal signaling pathway stimulating axon growth and neuroprotection.

4.4. Fast direct IL-4 receptor signaling on neurons

Immune-mediated increased intracellular Ca^{2+} levels result in axon dissection and neuronal soma degeneration (Siffrin, Radbruch et al. 2010). Ca^{2+} elevation is an early pathological sign of axonal dysfunction, causing axon swelling and leading to neuronal damage (McKinney, Lüthi et al. 1999, Nitsch, Pohl et al. 2004). Moreover, a continuous Ca^{2+} influx is sufficient to induce Wallerian degeneration due to the activation of Ca^{2+}-dependent proteases, which cause degradation of the cytoskeleton and the neurofilament (Schlaepfer and Zimmermann 1985). On the other hand, we were able to show that low physiological Ca^{2+} elevation caused by IL-4 signaling was able to act beneficial on neuronal outgrowth and regeneration. Moreover, we showed that by capturing the intracellular Ca^{2+} with the Ca^{2+}-chelator BAPTA-AM the effects of IL-4 on the F-actin changes abolished. Together these findings highlight the very delicate and crucial Ca^{2+} homeostasis in neurons, with pathological levels resulting in damage to the cell and physiological levels activating signaling pathways supporting outgrowth and repair. The beneficial effects of IL-4 include the prevention or repair of axon swelling indicating that it can reverse pathology caused by previous immune attacks.

The PKC family comprises the related PKCα through PKCι and is subdivided in three structurally and functionally distinguished groups of conventional (α, β1, β2, γ), novel (δ, ε, η) and the atypical (ζ, ι, λ) PKC. Of these, only the conventional PKC are sensitive to Ca^{2+} which binds to the archetypal C2 domain (Parker and Murray-Rust 2004). Of the conventional PKC, the γ subtype is of special interest in this thesis because of its exclusive expression in brain regions like the cerebral cortex and the spinal cord (Tanaka and Saito 1992). Moreover, it was shown that selectively blocking PKCα and β1 via intrathecal injection increased regeneration of lesioned dorsal column axons after SCI and promoted significant neurite outgrowth *in vitro* (Sivasankaran, Pei et al. 2004). Since PKCγ is a marker for CST, I chose PKCγ as the target protein for the IL-4R signal transduction. We were able to show a significant increase in PKCγ phosphorylation upon IL-4 treatment *in vitro*, supporting a positive effect on axonal outgrowth and regeneration.

Next, we showed that upon treatment with IL-4 PKC phosphorylated GAP-43, leading to the increased release of CaM from GAP-43 *in vitro*. The released CaM in combination with the

increase in intracellular Ca^{2+} activates Ca^{2+}/calmodulin-dependent protein kinase 2 (CaMKII) (Byth 2014). CaMKII is a serine/threonine kinase bound by F-actin at rest and is a major messenger and effector in early LTP (Okamoto, Bosch et al. 2009). Activation of CaMKII causes it to dissociate from actin and initiates the autophosphorylation, prolonging its activity (Byth 2014). CaMKII activation in axons allows remodeling of the cytoskeleton by triggering a signaling cascade resulting in the functional inactivation of cofilin (Laux, Fukami et al. 2000). Cofilin is an actin-binding protein severing F-actin filaments by depolymerization of actin into G-actin. While cofilin is modulating the actin equilibrium into actin depolymerization, there are also factors promoting actin polymerization. GAP-43 is known to activate signaling pathways promoting actin polymerization by regulation of $PI(4,5)P_2$ (Laux, Fukami et al. 2000). This is a second messenger regulating key actin binding proteins such as profilin and vinculin. Profilin is responsible for the elongation of F-actin and vinculin acts as a molecular clutch, organizing leading edge F-actin, generating extracellular matrix (ECM) traction and promoting focal adhesion (FA) formation and turnover (Thievessen, Thompson et al. 2013). Taken together, the phosphorylation of GAP-43 via IL-4 signaling initiates a two-way signaling promoting actin-polymerization and resulting in increased neurite outgrowth.

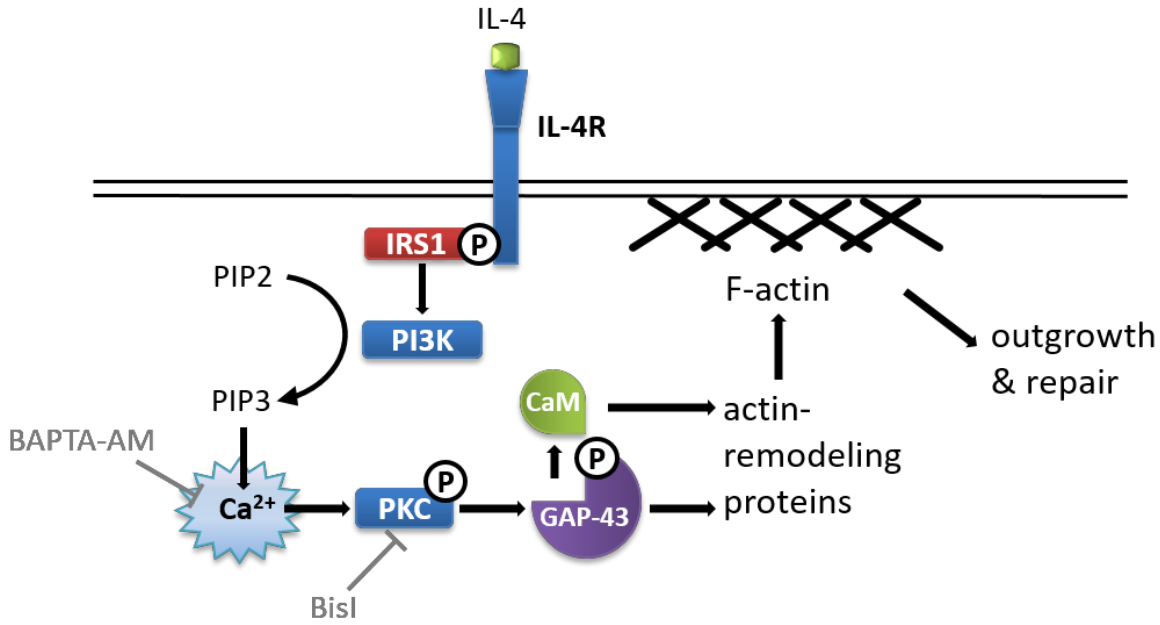

Figure 16: IL-4 receptor signaling in neurons.

Proposed neuronal IL-4R signaling: Binding of IL-4 to the IL-4R induces IRS1 phosphorylation and recruitment of PI3K. PI3K converts PIP2 to PIP3 resulting in Ca^{2+} influx, leading to the activation of PKC. PKC has been shown to phosphorylate GAP-43, which could be blocked by the addition of Bis1. Upon phosphorylation CaM is released from GAP-43 and PKC, GAP-43 and CaM stimulate actin-remodeling proteins, eventually leading to the polymerization of F-actin. The effects of IL-4 on the reorganization of F-actin is abolished with the co-treatment of BAPTA-AM. (Adapted from Vogelaar, Mandal, Lerch *et al*.)

4.5 Summary and Outlook

This thesis contributed to a study unraveling the fast and direct IL-4 receptor signaling in regard of protection and regeneration of neurons. In dissociated cortex neuron cultures, the necessary IL-4 receptor subunits to form the receptor Type I and II could be visualized utilizing immunocytochemistry methods. The findings indicate that docking proteins are recruited and key signaling molecules are phosphorylated in response to IL-4, leading to cytoskeletal remodeling. IL-4 treated cortex neurons could withstand a 24 h exposure to NMDA whereas PBS treated control cells showed a significant decrease in viability. In a novel *in vitro* neuronal outgrowth assay the treatment with IL-4 increased neurite outgrowth of neonatal cortex layer V explants by a two fold over the control group. Correspondingly it was shown that IL-4 treated EAE animals display marked increase in sprouting of neurites from the CST into the grey matter

with the anterograde tracer rhodamine-conjugated dextran, which was injected directly into the cortex. These findings implicate that IL-4 treated axons were able to overcome the natural CNS mechanisms that inhibit neurite sprouting and axonal growth. Accompanying this finding, IL-4 treated cortical layer V explants could overcome the inhibiting effect of a Nogo-A coating *in vitro*. Taken together, the findings of this thesis are of major neurological interest as the data show IL-4 exclusive effects neuroinflammatory axon injury. Targeting neuronal IL-4 signaling may lead the way to new therapeutic strategies to halt disability progression in MS and other related neurodegenerative diseases.

5. Bibliography

A. D. Keegan, K. N. (1994). "An IL-4 receptor region containing an insulin receptor motif is important for IL-4-mediated IRS-1 phosphorylation and cell growth." Cell **76**(5): 811-820.

Abe, K., et al. (2001). "Inhibition of Ras extracellular-signal-regulated kinase (ERK) mediated signaling promotes ciliary neurotrophic factor (CNTF) expression in Schwann cells." J Neurochem **77**.

Andrews, A. L., et al. (2002). "Kinetic analysis of the interleukin-13 receptor complex." J Biol Chem **277**(48): 46073-46078.

Biffo, S., et al. (1990). "B-50/GAP43 expression correlates with process outgrowth in the embryonic mouse nervous system." European Journal of Neuroscience **2**: 487-499.

Blaeser, F., et al. (2003). "Targeted inactivation of the IL-4 receptor alpha chain I4R motif promotes allergic airway inflammation." J Exp Med **198**(8): 1189-1200.

Byth, L. A. (2014). "Ca(2+)- and CaMKII-mediated processes in early LTP." Ann Neurosci **21**(4): 151-153.

Chapman, E. R., et al. (1990). "Characterization of the Calmodulin Binding Domain of Neuromodulin." J Biol Chem **266**(1): 207-213.

Chapman, E. R., et al. (1992). "Palmitylation of neuromodulin (GAP-43) is not required for phosphorylation by protein kinase C." J Biol Chem **267**(35): 25233-25238.

Chew, D. J., et al. (2012). "The challenges of long-distance axon regeneration in the injured CNS." Prog Brain Res **201**: 253-294.

Compston, A. and A. Coles (2008). "Multiple sclerosis." Lancet **372**.

Cummings, B. S. and R. G. Schnellmann (2004). "Measurement of cell death in mammalian cells." Curr Protoc Pharmacol **Chapter 12**: Unit 12 18.

David A. Ferrick, M. D. S., Thera Mulvania, Beryl Hsieh, Walter G. Ferlin & Heather Lepper (1994). "Differential production of interferon-γ and interleukin-4 in response to Th1- and Th2-stimulating pathogens by γδ T cells in vivo." Nature **373**: 255-257.

Davis, P. D., et al. (1989). "Potent selective inhibitors of protein kinase C." FEB **259**(1): 61-63.

De Graan, P. N., et al. (1990). "Evidence for the binding of calmodulin to endogenous B-50 (GAP-43) in native synaptosomal plasma membranes." J Neurochem.

DeLuca, G. C., et al. (2004). "Axonal loss in multiple sclerosis: a pathological survey of the corticospinal and sensory tracts." Brain **127**: 1009-1018.

Deshmukh, V. A., et al. (2013). "A regenerative approach to the treatment of multiple sclerosis." Nature **502**(7471): 327-332.

Dhand, R., et al. (1994). "PI 3-kinase is a dual specificity enzyme: autoregulation by an intrinsic protein-serine kinase activity." EMBO J **13**(3): 522-533.

Ellwardt, E., et al. (2016). "Understanding the Role of T Cells in CNS Homeostasis." Trends Immunol **37**(2): 154-165.

Ferreirinha, F., et al. (2004). "Axonal degeneration in paraplegin-deficient mice is associated with abnormal mitochondria and impairment of axonal transport." Journal of Clinical Investigation **113**(2): 231-242.

Franke, T. F., et al. (1997). "Direct regulation of the Akt proto-oncogene product by phosphatidylinositol-3,4-bisphosphate." Science **275**: 665-668.

Franklin, R. J. and C. Ffrench-Constant (2008). "Remyelination in the CNS: from biology to therapy." Nat Rev Neurosci **9**(11): 839-855.

Franklin, R. J., et al. (2012). "Neuroprotection and repair in multiple sclerosis." Nat Rev Neurol **8**(11): 624-634.

Freeley, M., et al. (2011). "Regulation of Protein Kinase C function by phosphorylation on conserved and non-conserved sites." Cell Signal **23**(5): 753-762.

Friese, M. A., et al. (2006). "The value of animal models for drug development in multiple sclerosis." Brain **129**(Pt 8): 1940-1952.

Friese, M. A., et al. (2014). "Mechanisms of neurodegeneration and axonal dysfunction in multiple sclerosis." Nat Rev Neurol **10**(4): 225-238.

Funfschilling, U., et al. (2012). "Glycolytic oligodendrocytes maintain myelin and long-term axonal integrity." Nature **485**(7399): 517-521.

Gallo, G., et al. (1997). "The trkA Receptor Mediates Growth Cone Turning toward a Localized Source of Nerve Growth Factor." J Neuroscience **17**(14): 5445-5454.

Gianinoa, S., et al. (1999). "Postnatal growth of corticospinal axons in the spinal cord of developing mice." Developmental Brain Research **112**(2): 189-204.

Giger, R. J., et al. (2010). "Guidance molecules in axon regeneration." Cold Spring Harb Perspect Biol **2**(7): a001867.

Hajieva, P., et al. (2018). "The role of Plasma Membrane Calcium ATPases (PMCAs) in neurodegenerative disorders." Neurosci Lett **663**: 29-38.

Hasan, M., et al. (2016). "Increased levels of brain serotonin correlated with MMP-9 activity and IL-4 levels resulted in severe experimental autoimmune encephalomyelitis (EAE) in obese mice." Neuroscience **319**: 168-182.

Hechler, D., et al. (2010). "Differential regulation of axon outgrowth and reinnervation by neurotrophin-3 and neurotrophin-4 in the hippocampal formation." Exp Brain Res **205**(2): 215-221.

Heller, N. M., et al. (2012). The Type I and Type II Receptor Complexes for IL-4 and IL-13 Differentially Regulate Allergic Lung Inflammation. Allergic Diseases - Highlights in the Clinic, Mechanisms and Treatment. C. Pereira, InTech.

Herz, J., et al. (2010). "Neurodegeneration in autoimmune CNS inflammation." Exp Neurol **225**(1): 9-17.

Hsieh CS1, H. A., Gold JS, O'Garra A, Murphy KM. (1992). "Differential regulation of T helper phenotype development by interleukins 4 and 10 in an alpha beta T-cell-receptor transgenic system." Proc Natl Acad Sci U S A **89**: 6065-6069.

Huebner, E. A., et al. (2011). "A multi-domain fragment of Nogo-A protein is a potent inhibitor of cortical axon regeneration via Nogo receptor 1." J Biol Chem **286**(20): 18026-18036.

Huijbregts, S. C. J., et al. (2004). "Differences in cognitive impairment of relapsing remitting, secondary, and primary progressive MS." Neurology **62**(2): 335-339.

Johnston, J. A., et al. (1994). "Phosphorylation and activation of the Jak-3 Janus kinase in response to interleukin-2." Nature **370**(14).

Jolivel, V., et al. (2013). "Modulation of dendritic cell properties by laquinimod as a mechanism for modulating multiple sclerosis." Brain **136**(Pt 4): 1048-1066.

K. Izuhara, K. A., S. Yasunaga. (2002). "IL-4 and IL-13: Their Pathological Roles in Allergic Diseases and their Potential in Developing New Therapies." Curr Drug Targets **1**(3).

Kammer, W., et al. (1996). "Homodimerization of interleukin-4 receptor alpha chain can induce intracellular signaling." J Biol Chem **271**(39): 23634-23637.

Katz, F., et al. (1985). "Nerve growth cones isolated from fetal rat brain III, Calcium-dependent protein phosphorylation." Journal of Neuroscience **5**(6): 1402-1411.

Kevenaar, J. T. and C. C. Hoogenraad (2015). "The axonal cytoskeleton: from organization to function." Front Mol Neurosci **8**: 44.

Kraus, S. H., et al. (2014). "Cladribine exerts an immunomodulatory effect on human and murine dendritic cells." Int Immunopharmacol **18**(2): 347-357.

Kriegstein, A. R. and M. A. Dichter (1983). "Morphological classification of rat cortical neurons in cell culture." J Neurosci **3**(8): 1634-1647.

Laatsch, R. H., et al. (1962). "The encephalomyelitic activity of myelin isolated by ultracentrifugation." J Exp Med **115**(4).

Lai, T. W., et al. (2014). "Excitotoxicity and stroke: identifying novel targets for neuroprotection." Prog Neurobiol **115**: 157-188.

Larochelle, C., et al. (2016). "Secondary Progression in Multiple Sclerosis: Neuronal Exhaustion or Distinct Pathology?" Trends Neurosci **39**(5): 325-339.

Laux, T., et al. (2000). "Gap43, Marcks, and Cap23 Modulate Pi(4,5p)2 at Plasmalemmal Rafts, and Regulate Cell Cortex Actin Dynamics through a Common Mechanism." J Cell Biol **149**(7): 1455-1472.

Lee, F. S. and M. V. Chao (2001). "Activation of Trk neurotrophin receptors in the absence of neurotrophins." Proc Natl Acad Sci U S A **98**(6): 3555-3560.

Leea, S. E., et al. (1998). "Expression of nerve growth factor in the dorsal root ganglion after peripheral nerve injury." Brain Res **796**(1-2).

Lesuisse, C. and L. J. Martin (2002). "Long-term culture of mouse cortical neurons as a model for neuronal development, aging, and death." J Neurobiol **51**(1): 9-23.

Liu, Y., et al. (2005). "Ryk-mediated Wnt repulsion regulates posterior-directed growth of corticospinal tract." Nat Neurosci **8**(9): 1151-1159.

Lowenthal, J. W., et al. (1988). "Expression of high affinity receptors for murine interleukin 4 (BSF-1) on hemopoietic and nonhemopoietic cells." J Immunol **140**: 456-464.

Lu, C., et al. (2008). "Pertussis toxin induces angiogenesis in brain microvascular endothelial cells." J Neurosci Res **86**(12): 2624-2640.

Lublin, F. D. and S. C. Reingold (1996). "Defining the clinical course of multiple sclerosis." Neurology **46**(4).

Mahoney, C. W., et al. (1995). "Phosphorylation of MARCKS, neuromodulin, and neurogranin by protein kinase C exhibits differential responses to diacylglycerols." Cell Signal **7**(7): 679-685.

Manev, H., et al. (1989). "Delayed increase of Ca2+ influx elicited by glutamate: role in neuronal death." Molecular Pharmacology **36**(1).

Maragakis, N. J. and J. D. Rothstein (2006). "Mechanisms of Disease: astrocytes in neurodegenerative disease." Nat Clin Pract Neurol **2**(12): 679-689.

Markus, A. (2002). "Neurotrophic factors and axonal growth." Curent Opinion in Neurobiology **12**(5): 523-531.

McKinney, R. A., et al. (1999). "Selective glutamate receptor antagonists can induce or prevent axonal sprouting in rat hippocampal slice cultures." PNAS **96**(20).

Meberg, P. J., et al. (1995). "Protein FI/GAP-43 and PKC gene expression patterns in hippocampus are altered 1-2 h after LTP." Mol Brain Res **34**: 343-346.

Mi, S., et al. (2007). "LINGO-1 antagonist promotes spinal cord remyelination and axonal integrity in MOG-induced experimental autoimmune encephalomyelitis." Nat Med **13**(10): 1228-1233.

Miyajima, A., et al. (1992). "Cytokine Receptors and signal transduction." Annu. Rev. Immunol **10**: 295-331.

Miyazaki, T., et al. (1994). "Functional activation of Jak1 and Jak3 by selective association with IL-2 receptor subunits." Science **266**.

Murata, T., et al. (1996). "IL-13 induces phosphorylation and activation of JAK2 Janus kinase in human colon carcinoma cell lines: similarities between IL-4 and IL-13 signaling." J Immunol **156**(8): 2972-2978.

Nash, M., et al. (2009). "Central nervous system regeneration inhibitors and their intracellular substrates." Mol Neurobiol **40**(3): 224-235.

Nelms, K., et al. (1999). "The IL-4 receptor: signaling mechanisms and biologic functions." Annu Rev Immunol **17**: 701-738.

Nicholls, D. G. (2004). "Mitochondrial Dysfunction and Glutamate Excitotoxicity Studied in Primary Neuronal Cultures." Current Molecular Medicine **4**(2).

Nicholson-Fish, J. C., et al. (2016). "Phosphatidylinositol 3-Kinase Couples Localised Calcium Influx to Activation of Akt in Central Nerve Terminals." Neurochem Res **41**(3): 534-543.

Nikic, I., et al. (2011). "A reversible form of axon damage in experimental autoimmune encephalomyelitis and multiple sclerosis." Nat Med **17**(4): 495-499.

Nishizuka, Y. (1995). "Protein kinase C and lipid signaling for sustained cellular responses." FASEB **9**(7): 484-496.

Nitsch, R., et al. (2004). "Direct impact of T cells on neurons revealed by two-photon microscopy in living brain tissue." J Neurosci **24**(10): 2458-2464.

Norenberg, M. D. and K. V. Rao (2007). "The mitochondrial permeability transition in neurologic disease." Neurochem Int **50**(7-8): 983-997.

Obrenovitch, T. B. and J. Urenjak (1997). "Is High Extracellular Glutamate the Key to Excitotoxicity in Traumatic Brain Injury?" J Neurotrauma **14**(10).

Oestreicher, A. B., et al. (1997). "B-50, the growth associated protein-43: modulation of cell morphology and communication in the nervous system." Prog Neurobiol **53**(6): 627-686.

Okamoto, K., et al. (2009). "The roles of CaMKII and F-actin in the structural plasticity of dendritic spines: a potential molecular identity of a synaptic tag?" Physiology (Bethesda) **24**: 357-366.

Park, E., et al. (2004). "The role of excitotoxicity in secondary mechanisms of spinal cord injury: a review with an emphasis on the implications for white matter degeneration." J Neurotrauma **21**(6): 754-774.

PArk, L. S., et al. (1987). "Characterization of the human B cell stimulatory factor 1 receptor." J Exp Med **166**: 476-488.

Parker, P. J. and J. Murray-Rust (2004). "PKC at a glance." J Cell Sci **117**(Pt 2): 131-132.

Payne, N. L., et al. (2012). "Early intervention with gene-modified mesenchymal stem cells overexpressing interleukin-4 enhances anti-inflammatory responses and functional recovery in experimental autoimmune demyelination." Cell Adh Migr **6**(3): 179-189.

Pernet, V. and M. E. Schwab (2012). "The role of Nogo-A in axonal plasticity, regrowth and repair." Cell Tissue Res **349**(1): 97-104.

Planche, V., et al. (2016). "Cognitive impairment in a population-based study of patients with multiple sclerosis: differences between late relapsing-remitting, secondary progressive and primary progressive multiple sclerosis." Eur J Neurol **23**(2): 282-289.

R A Seder, W. E. P., M M Davis, B Fazekas de St Groth (1992). "The presence of interleukin 4 during in vitro priming determines the lymphokine-producing potential of CD4+ T cells from T cell receptor transgenic mice." J. Exp. Med. **176**: 1091-1098.

Raivich, G. and G. W. Kreutzberg (1993). "Peripheral nerve regeneration: role of growth factors and their receptors." Int J Dev Neurosci **11**(3).

Ramakers, G. M. J. (1995). "Temporal differenoes in the phosphorylation state of pre- and postsynaptic protein kinase C substrates B-50/GAP-43 and neurogranin during long term potentiation." J Biol Chem **270**(9): 13892-13898.

Ransohoff, R. M. (2012). "Animal models of multiple sclerosis: the good, the bad and the bottom line." Nat Neurosci **15**(8): 1074-1077.

Rivers, T. M., et al. (1933). "Observations on attempts to produce acute disseminated encephalomyelitis in monkeys." JEM.

Russell, S. M., et al. (1994). "Interaction of IL-2R beta and gamma c chains with Jak1 and Jak3: implications for XSCID and XCID." Science **266**.

S Dubucquoi, P. D., A Janin, O Klein, M Goldman, J Tavernier, A Capron, M Capron (1994). "Interleukin 5 synthesis by eosinophils: association with granules and immunoglobulin-dependent secretion." J. Exp. Med. **179**: 703-708.

Saito, N. and Y. Shirai (2002). "Protein kinase C gamma (PKC gamma): function of neuron specific isotype." J Biochem **132**(5): 683-687.

Sawcer, S. (2011). "Genetic risk and a primary role for cell-mediated immune mechanisms in multiple sclerosis." Nature **476**: 214-219.

Schlaepfer, W. W. and U. Zimmermann (1985). "Calcium-activated proteolysis of intermediate filaments." Ann N Y Acad Sci: 552-562.

Seder, R. A. and W. E. Paul (1994). "Acquisition of lymphokine-producing phenotype by CD4+ T cells." Annu Rev Immunol **12**: 635-673.

Sheu, J. Y., et al. (2000). "Differential patterns of ERK and STAT3 phosphorylation after sciatic nerve transection in the rat." Exp Neurol **166**(2): 392-402.

Sholl-Franco, A., et al. (2009). "Interleukin-4 as a neuromodulatory cytokine: roles and signaling in the nervous system." Ann N Y Acad Sci **1153**: 65-75.

Siffrin, V., et al. (2010). "In vivo imaging of partially reversible th17 cell-induced neuronal dysfunction in the course of encephalomyelitis." Immunity **33**(3): 424-436.

Sivasankaran, R., et al. (2004). "PKC mediates inhibitory effects of myelin and chondroitin sulfate proteoglycans on axonal regeneration." Nat Neurosci **7**(3): 261-268.

Smerz-Bertling, C. and A. Duschl (1995). "Both interleukin 4 and interleukin 13 induce tyrosine phosphorylation of the 140-kDa subunit of the interleukin 4 receptor." J Biol Chem **270**: 966-970.

Snow, D. M., et al. (1990). "Sulfated proteoglycans in astroglial barriers inhibit neurite outgrowth in vitro." Exp Neurol **109**(1): 111-130.

Steward, O., et al. (2004). "The dorsolateral corticospinal tract in mice: an alternative route for corticospinal input to caudal segments following dorsal column lesions." J Comp Neurol **472**(4): 463-477.

Sun, X. I., et al. (1991). "Structure of the insulin receptor substrate IRS-1 defines a unique signal transduction protein." Nature **352**: 73-77.

Sun, X. I., et al. (1995). "Role of IRS-2 in insulin and cytokine signalling." Nature **377**: 173-177.

Tanaka, C. and N. Saito (1992). "Localization of subspecies of protein kinase C in the mammalian central nervous system." Neurochem International **21**(4): 499-512.

Thievessen, I., et al. (2013). "Vinculin-actin interaction couples actin retrograde flow to focal adhesions, but is dispensable for focal adhesion growth." J Cell Biol **202**(1): 163-177.

Thoenen, H. (1995). "Neurotrophins and neuronal plasticity." Science.

Tompkins, S. M., et al. (2002). "De Novo Central Nervous System Processing of Myelin Antigen Is Required for the Initiation of Experimental Autoimmune Encephalomyelitis." The Journal of Immunology **168**(8): 4173-4183.

Tuohy, V. K., et al. (1992). "Myelin proteolipid protein: minimum sequence requirements for active induction of autoimmune encephalomyelitis in SWR/J and SJL/J mice." JNI **39**(1-2): 67-74.

Tutuncu, M., et al. (2013). "Onset of progressive phase is an age-dependent clinical milestone in multiple sclerosis." Mult Scler **19**(2): 188-198.

Vogelaar, C. F., et al. (2003). "Homeobox gene expression in adult dorsal root ganglia during sciatic nerve regeneration: is regeneration a recapitulation of development?" Eur J Pharmacol **480**(1-3): 233-250.

Vogelaar, C. F., et al. (2018). "Fast direct neuronal signaling via the IL-4 receptor as therapeutic target in neuroinflammation." **10**(430).

Vogt, J., et al. (2009). "Lower motor neuron loss in multiple sclerosis and experimental autoimmune encephalomyelitis." Ann Neurol **66**(3): 310-322.

Walsh, J. T., et al. (2015). "MHCII-independent CD4+ T cells protect injured CNS neurons via IL-4." J Clin Invest **125**(2): 699-714.

William, B. J., et al. (2001). "Leukemia Inhibitory Factor Determines the Growth Status of Injured Adult Sensory Neurons." The Journal of Neuroscience **21**(18): 7161-7170.

Witthuhn, B. A. (1994). "Involvement of the Jak-3 Janus kinase in signalling by interleukins 2 and 4 in lymphoid and myeloid cells." Nature **370**(14).

Woolf, C. J., et al. (1992). "Denervation of the motor endplate results in the rapid expression by terminal Schwann cells of the growth-associated protein GAP-43." J Neurosci **12**(10): 3999-4010.

Wright, K. T., et al. (2007). "Bone marrow stromal cells stimulate neurite outgrowth over neural proteoglycans (CSPG), myelin associated glycoprotein and Nogo-A." Biochem Biophys Res Commun **354**(2): 559-566.

Yin, T. (1995). "Interleukin-9 induces tyrosine phosphorylation of insulin receptor substrate-1 via JAK tyrosine kinases." J Biol Chem **270**(35): 20497-20502.

Zhao, X., et al. (2015). "Neuronal Interleukin-4 as a Modulator of Microglial Pathways and Ischemic Brain Damage." J Neurosci **35**(32): 11281-11291.

Zipp, F. and O. Aktas (2006). "The brain as a target of inflammation: common pathways link inflammatory and neurodegenerative diseases." Trends Neurosci **29**(9): 518-527.

Zipp, F., et al. (2013). "Identification of inflammatory neuronal injury and prevention of neuronal damage in multiple sclerosis: hope for novel therapies?" JAMA Neurol **70**(12): 1569-1574.

Zurawski, S. M., et al. (1993). "Receptors for interleukin-13 and interleukin-4 are complex and share a novel component that functions in signal transduction." EMBO J **12**(7): 2663-2670.

Zwiers, H., et al. (1976). "ACTH, cyclic nucleotides, and brain protein phosphorylation in vitro." Neurochem Res: 669-677.

6. Abbreviations

°C	degree Celsius
µ	micro
µg	microgram
µl	microliter
µm	micrometer
A	ampere
ATP	adenosine triphosphate
BAPTA	1,2-Bis(2-aminophenoxy)ethane-N,N,N′,N′-tetraacetic acid
BBB	blood brain barrier
BSA	bovine serum albumin
Ca^{2+}	calcium
$CaCl_2$	calcium chloride
CamKIIα	calcium/calmodulin-dependent protein kinase II alpha
CD	cluster of differentiation
CFA	complete Freud's adjuvant
CNS	central nervous system
CO_2	carbon dioxide
CSF	cerebrospinal fluid
CST	corticospinal tract
DAPI	4′,6-Diamidino-2-phenylindole dihydrochloride
DIV	days *in vitro*
DMSO	dimethyl sulfoxide
EAE	experimental autoimmune encephalomyelitis
EDTA	ethylenediaminetetraacetic acid
e.g.	exempli gratia
EtOH	ethanol
g	earth gravity
GAP-43	growth associated protein 43
h	hour
HBSS	Hank's balanced salt solution
HCl	hydrochloric acid
HEPES	N-(2-Hydroxyethyl)piperazine-N′-(2-ethanesulfonic acid)
HS	horse serum
IGF-1	insulin-like growth factor 1
IL	interleukin
IRS-1	insulin receptor substrate 1
LTD	long term depression
LTP	long term potentiation
kDa	kilodalton
KO	knock out
min	minutes

ml	milliliter
mM	millimolar
MOG	myelin oligodendrocyte glycoprotein
MRI	magnetic resonance imaging
MS	multiple sklerosis
NaCl	sodium chloride
ng	nanogram
NH_4Cl	ammonium chloride
PBS	Phosphate-buffered saline
PDL	Poly-D-lysine
PFA	paraformaldehyde
PKC	protein kinase C
PP	primary progessive
PLP	proteolipid protein
PTX	pertussis toxin
rh	recombinant human
RPM	revolutions per minute
RT	room temperatur
RR	relapsing-remitting
SDS	sodium dodecyl sulfate
SP	secondary progressive
TGF	transforming growth factor
T_H	T helper
TLR	Toll-like receptor
TNF	tumor necrosis factor
Tx	Triton-x
V	volt
WT	wild type

7. Index of Illustrations and Tables

.

Curriculum vitae

Steffen Lerch

Studies

06/2013 – 06/2018	**PhD student at the Neuroimmunology Department, Johannes Gutenberg University Medical Center Mainz** PhD thesis: Interleukin-4 receptor pathway in neurons Side project: Characterization of dendritic cells, Th1 and Th17 cells in human MS and murine EAE **Skills**: immunocytochemistry, immunostaining, laser microscopy (confocal, 2photon imaging), immuno assays, cell culture (murine and human), induced stem cell culture (cell lines), transfection, western blot, immunoprecipitation
10/2012 – 06/2013	**Diploma thesis at the Institute of Molecular Genetic, Johannes Gutenberg University of Mainz** Analysis of the serin/threoninekinasis 33-gene (Stk33) in the ostrich genome (*Stuthio camelus*); Next Generation Sequencing **Skills:** bacterial transformation, cloning, primer design, PCR, electrophoresis, Sanger sequencing, pyrosequencing, NGS
04/2007 – 04/2013	**Studies in Biology, Johannes Gutenberg University, Mainz** Main subjects: Genetics, pharmacology and toxicology, zoology
2001 – 2004	General qualification for university, Alfred-Delp High School, Dieburg, Final exams in biology and arts.

Professional experience

11/2012 – 12/2012	**Keys Marine Laboratory, Florida (USA), Supervisor,** project planning and execution with young scientists
01/2012 – 02/2012	**Institute of Zoology, Johannes Gutenberg-University, Mainz, Internship** Expression of mutated fish fetuin proteins Purification and analyzation of mutated fish fetuin proteins
11/2011 – 12/2011	**Keys Marine Laboratory, Florida (USA), Supervisor,** attitude survey and characterization of marine organisms
08/2011 – 10/2011	**Institute of Molecular Genetics, Johannes Gutenberg-University, Mainz, Internship,** Analyzing the expression pattern of bovine mesenchymal stem cells, microarray assays, isolating and vector-cloning of the stem cell transcription factor SoxII
03/2011	**Institute of Zoology, Johannes Gutenberg-University, Mainz, Internship,** Preparation and immunostaining of selected proteins in organs of mice; sample preparation and scanning electron microscopy of eye specimen
10/2009	**Institute of Toxicology, University Medical Center, Mainz, Internship,** Pharmacology and Toxicology Dosage-effect relation of different pharmaceutical products - *in vivo* and *in silico* testing

Skills

Languages	German (native speaker), English (fluent), French (basic knowledge)
Computing	Microsoft Office (Word, Excel, PowerPoint), GraphPad Prism 6, Photoshop, CLC Genomics Workbench, FlowJo, Leica LAS AF
	Qualified for laboratory animal handling and laboratory safety (FELASA B)

Publications

Fast direct neuronal signaling via the IL-4 receptor as therapeutic target in neuroinflammation.C. F. Vogelaar*, Shibajee Mandal*, **Steffen Lerch***, Katharina Birkner, Jerome Birkenstock, Ulrike Bühler, Andrea Schnatz, Cedric S. Raine, Stefan Bittner, Johannes Vogt, Jonathan Kipnis, Frauke Zipp
Science Translational Medicine, 2018

PMID: 29491183

FTY720 (fingolimod) treatment tips the balance towards less immunogenic antigen-presenting cells in patients with multiple sclerosis. Luessi F., Kraus S., Trinschek B., Lerch S., Ploen R., Paterka M., Roberg T., Poisa-Beiro L., Klotz L., Wiendl H., Bopp T., Jonuleit H., Jolivel V., Zipp F., Witsch, E. Multiple Sclerosis. 2015

PMID: 25732840

The serine/threonine kinase 33 is present and expressed in palaeognath birds but has become a unitary pseudogene in neognaths about 100 million years ago. T. Lautwein, S. Lerch, D. Schäfer., Schmidt ER.
BMC Genomics 2015

PMID: 26199010

Cladribine exerts an immunomodulatory effect on human and murine dendritic cells. Kraus SHP, Luessi F, Trinschek B, Lerch S; Hubo M., Poisa-Beiro L., Paterka M., Jonuleit H., Zipp F., Jolivel V.
Int Immunopharmacol. 2013

PMID: 24316255